HOLOGIC®
The Science of Sure

Powerful images. **Clear answers.**

Manage Patient's concerns about Atypical Femur Fracture*

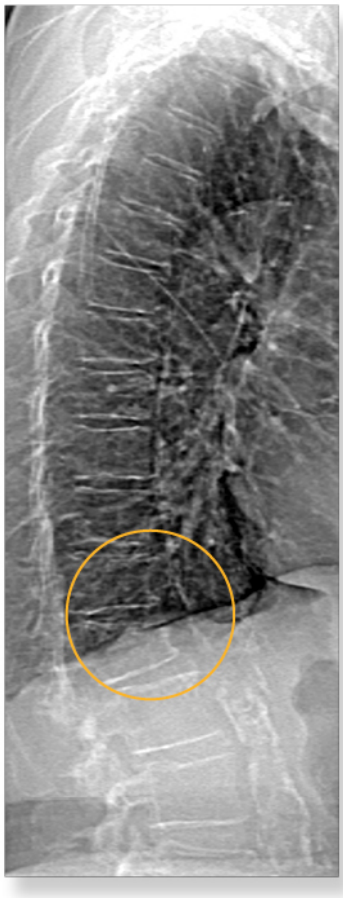

Vertebral Fracture Assessment – a critical part of a complete fracture risk assessment

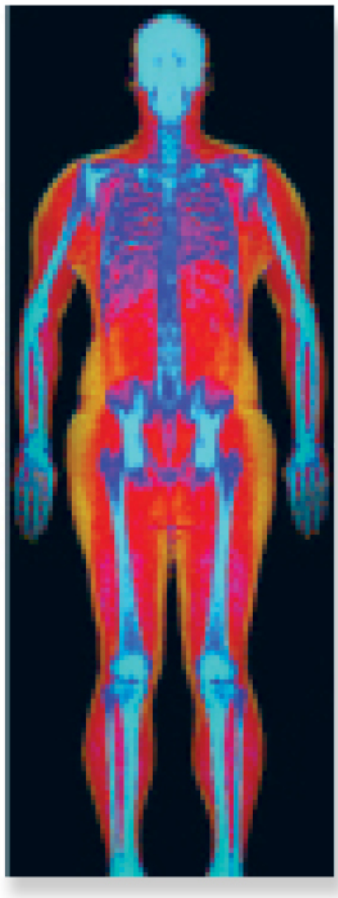

Advanced Body Composition® Assessment – the power to see what's inside

Contact your Hologic rep today at BSHSalesSupportUS@hologic.com

*Incomplete Atypical Femur Fractures imaged with a Hologic densitometer, courtesy of Prof. Cheung, University of Toronto

www.hologic.com | dxaperformance.com | 1.800.442.9892

RESEARCH ARTICLE

JBMR®

The Multifarious Functions of Leukotrienes in Bone Metabolism

Flávia Amadeu de Oliveira,[1,2] Cintia K. Tokuhara,[1,2] Vimal Veeriah,[3] João Paulo Domezi,[1] Mariana R. Santesso,[1] Tania M. Cestari,[1] Talita M.O. Ventura,[1] Adriana A. Matos,[1,4] Thiago Dionísio,[1] Marcel R. Ferreira,[5] Rafael C. Ortiz,[1] Marco A.H. Duarte,[1] Marília A.R. Buzalaf,[1] José B. Ponce,[6,7] Carlos A. Sorgi,[8] Lucia H. Faccioli,[8] Camila Peres Buzalaf,[1] and Rodrigo Cardoso de Oliveira[1]

[1]Bauru School of Dentistry, University of São Paulo, Bauru, SP, Brazil
[2]Human Genetics Program, Sanford Children's Health Research Center, Sanford Burnham Prebys Medical Discovery Institute, San Diego, CA, USA
[3]Institute for Regenerative Medicine, University of Zürich, Zürich, Switzerland
[4]Ribeirão Preto Medical School, University of São Paulo, Ribeirão Preto, SP, Brazil
[5]Institute of Biosciences, São Paulo State University-UNESP, Botucatu, SP, Brazil
[6]Department of Medicine, University Center of Adamantina, Adamantina, SP, Brazil
[7]Department of Medicine, Faculdades de Dracena, Dracena, SP, Brazil
[8]School of Pharmaceutical Sciences of Ribeirão Preto, University of São Paulo, Ribeirão Preto, SP, Brazil

ABSTRACT

Leukotrienes (LTs) are derived from arachidonic acid metabolism by the 5-lipoxygenase (5-LO) enzyme. The production of LTs is stimulated in the pathogenesis of rheumatoid arthritis (RA), osteoarthritis, and periodontitis, with a relevant contribution to bone resorption. However, its role in bone turnover, particularly the suppression of bone formation by modulating the function of osteoclasts and osteoblasts, remains unclear. We investigated the effects of LTs on bone metabolism and their impact on osteogenic differentiation and osteoclastogenesis using a 5-LO knockout (KO) mouse model. Results from micro-computed tomography (μCT) analysis of femur from 8-week-old 5-LO-deficient mice showed increased cortical bone and medullary region in females and males and decreased trabecular bone in females. In the vertebra, we observed increased marrow area in both females and males 5-LO KO and decreased trabecular bone only in females 5-LO KO. Immunohistochemistry (IHC) analysis showed higher levels of osteogenic markers tissue-nonspecific alkaline phosphatase (TNAP) and osteopontin (OPN) and lower expression of osteoclastogenic marker tartrate-resistant acid phosphatase (TRAP) in the femurs of 5-LO KO mice versus wild-type (WT). Alkaline phosphatase activity and mineralization assay results showed that the 5-LO absence enhances osteoblasts differentiation and mineralization but decreases the proliferation. Alkaline phosphatase (ALP), Bglap, and Sp7 gene expression were higher in 5-LO KO osteoblasts compared to WT cells. Eicosanoids production was higher in 5-LO KO osteoblasts except for thromboxane 2, which was lower in 5-LO–deficient mice. Proteomic analysis identified the downregulation of proteins related to adenosine triphosphate (ATP) metabolism in 5-LO KO osteoblasts, and the upregulation of transcription factors such as the adaptor-related protein complex 1 (AP-1 complex) in long bones from 5-LO KO mice leading to an increased bone formation pattern in 5-LO–deficient mice. We observed enormous differences in the morphology and function of osteoclasts with reduced bone resorption markers and impaired osteoclasts in 5-LO KO compared to WT osteoclasts. Altogether, these results demonstrate that the absence of 5-LO is related to the greater osteogenic profile. © 2023 The Authors. *Journal of Bone and Mineral Research* published by Wiley Periodicals LLC on behalf of American Society for Bone and Mineral Research (ASBMR).

KEY WORDS: 5-LIPOXYGENASE; BONE LOSS; INFLAMMATORY DISEASES; LEUKOTRIENES; OSTEOBLASTS; OSTEOCLASTOGENESIS

Received in original form January 18, 2023; revised form May 28, 2023; accepted May 31, 2023.
Address correspondence to: Flávia Amadeu de Oliveira, PhD, Sanford Burnham Prebys, 10901 N. Torrey Pines Road, La Jolla, CA 92037, USA. E-mail: famadeu@sbpdiscovery.org
Additional Supporting Information may be found in the online version of this article.
Journal of Bone and Mineral Research, Vol. 38, No. 8, August 2023, pp 1135–1153.

DOI: 10.1002/jbmr.4867

Introduction

The mechanisms by which bone modulation occurs are complex and involve interactions between cells, local and systemic factors.[1,2] Imbalanced bone formation and bone resorption are correlated to various diseases. Chronic inflammatory conditions are associated with osteoporosis and increased bone fragility. During inflammation, various immune cell populations are activated to produce inflammatory cytokines. Those molecules can activate the bone degradation cascade and impair bone formation.[3] Therefore, the chronic inflammatory process induces increasing osteopenia.[4]

In addition to cytokines, several other factors are involved in the regulation of bone homeostasis such as hormones, messenger molecules, and lipid mediators.[5-7] In this context, leukotrienes (LTs) are lipid mediators produced from the action of the enzyme 5-lipoxygenase (5-LO) with a relevant role in the inflammatory response.[8] They are products of the arachidonic acid (AA) metabolism and are released after cellular activation by toxins,[9] immune complexes,[10] and soluble mediators.[11]

LTs comprise LTB_4 and cysteinyl leukotrienes (cysLTs), such as LTC_4, LTD_4, and LTE_4. They mediate autocrine or paracrine signaling by binding to the G protein-coupled transmembrane type receptors (GPCRs.) LTB_4 is a potent chemotactic mediator responsible for leukocyte recruitment and amplification of the inflammatory response. It is mainly produced by neutrophils, macrophages, and mast cells[12] and is highly present in synovial fluid and serum of patients with inflammatory diseases such as rheumatoid arthritis (RA),[13] whereas cysLTs are known for their bronchoconstrictor properties.[14,15] However, little is known about the biological effects of LTs on bone homeostasis.

Previous reports showed the importance of LTB_4 and LTD_4 in bone remodeling and their ability to stimulate osteoclastogenesis and osteoclast function.[16,17] These inflammatory mediators are responsible for the inhibition of bone formation by reducing the mineralized nodule formation with decreased alkaline phosphatase activity in murine calvariae osteoblasts leading to impairment of osteoblast differentiation and function.[18] The 5-LO pathway in bone resorption became evident with the presence of LTB_4 receptor (BLT1) in osteoclasts and that bone cells were able to produce LTs.[19-23] In vitro studies have shown that LTB_4 increases bone resorption in murine cells[16] and promotes osteoclast formation from human peripheral blood mononuclear cells, in a receptor activator of nuclear factor κB ligand (RANKL)-independent manner.[22,24]

Inhibition of the 5-LO enzyme attenuates inflammation and bone resorption in lipopolysaccharide (LPS)-induced periodontal disease, suggesting the role of LTs as an inducer of osteodegenerative diseases.[25] LTB_4 inhibited alkaline phosphatase activity in a dose-dependent manner in human osteoarthritis subchondral osteoblasts.[21]

Several studies demonstrated LTs as a negative regulator of bone in 5-LO knockout (KO) mice, suggesting its role as an inducer of osteodegenerative diseases, such as osteoporosis,[26] osteoarthritis,[21] periodontitis,[27,28] and RA.[13] In the present study, we demonstrated altered bone phenotypes in mice lacking 5-LO and analyzed the molecular profile of osteoblasts and osteoclasts in these bones. In this sense, an understanding of the mechanisms orchestrated by inflammatory mediators that lead to different biological responses in the skeletal tissue is of great importance and may help the development of treatments for bone loss associated with inflammatory diseases, orthopedic and dental trauma, or even bone malignancies.

Materials and Methods

Animals

Eight-week-old female and male homozygous for the *Alox5*^{tm1Fun}, also called 5-lipoxygenase knockout (5-LO KO), in the background of 129S2/Sv mice, and 129/Sv wild-type (WT) control mice were obtained from The Jackson Laboratory (Bar Harbor, ME, USA) and maintained/bred in the vivarium at the University of São Paulo. Eight-week-old mice were used for in vivo experiments and 7-day-old pups, for the in vitro experiments. The animal room had a 12 hour light/dark cycle and certified Envigo Teklad Global Rodent Diets® were available *ad libitum* during acclimation and throughout the study. We did not observe pain or distress. 5-LO KO mice are viable and apparently live a normal lifespan, so we did not have any limitations of this model for this study. Genotyping was performed by standard polymerase chain reaction (PCR) method. All experiments were approved and conducted according to the guidelines of the Ethics Committee on Animal Education and Research of the University of São Paulo, Bauru School of Dentistry (CEEPA Proc. #005/2017) and Animals in Research: Reporting In Vivo Experiments (ARRIVE).

Micro–computed tomography

Femurs and vertebrae images were acquired through Sky Scan 1174 μCT scanner (Bruker, Kontich, Belgium) (X-ray 50 kV and 800 μA) with a voxel size (volume and pixel) of 7.7 μm for the femur and 14.1 μm for the fifth lumbar vertebra (L_5). The following parameters were evaluated using the CT-An software: Bone volume (BV), total tissue volume (TV), bone volume/total volume (BV/TV), bone surface (BS), bone surface/total volume (BS/TV), specific bone surface (BS/BV), trabecular number (Th.N), trabecular thickness (Th.Th), and trabecular separation (Th.Sp). A total of 50 slices from the proximal to the distal femur growth plate were analyzed. For the cortical bone, 50 slices of the mid-femur of each bone were used to quantify cortical BV/TV and TV of the cortical bone. For the trabecular bone of vertebrae, 100 slices were analyzed from the proximal to the distal growth plate.

Immunofluorescence analysis

Immunofluorescence (IF) was performed on tissue sections of decalcified formalin-fixed and paraffin-embedded (FFPE) femurs and vertebrae from 5-LO KO and WT mice. Sections were permeabilized with triton X-100, blocked with 5% donkey serum followed by overnight incubation with tartrate-resistant acid phosphatase (TRAP) (rabbit anti-TRAP/CD40L; Abcam, Cambridge, MA, USA; #ab2391-Abcam) and osteopontin (OPN) (goat anti-OPN; Sigma-Aldrich, St. Louis, MO, USA; #O7635-Sigma-Aldrich) primary antibodies, and followed by incubation with Alexa Fluor 647 goat anti-rabbit (Invitrogen, Carlsbad, CA, USA; #A27040-Invitrogen) and Alexa Fluor 488 donkey anti-goat (#A11055-Invitrogen) as secondary antibodies, respectively. Nuclei were counterstained with DAPI (4′,6-diamidino-2-phenylindole, dihydrochloride). Images were acquired using the Keyence BZ-X800 fluorescence microscope at magnification ×20. Fluorescence intensity was quantified by ImageJ software (NIH, Bethesda, MD, USA; https://imagej.nih.gov/ij/).

Immunohistochemistry

Immunostaining was done in the femurs of females and males for tissue nonspecific alkaline phosphatase (TNAP) and OPN, and in femurs of females for TRAP, from 5-LO KO and WT mice, by the avidin-biotin-peroxidase complex (ABC) method (Vector Labs, Burlingame, CA, USA). SuperBlock in phosphate-buffered saline (PBS) (Life Technologies, Waltham, MA, USA) was used for blocking the following primary antibodies for TNAP (rat anti-TNAP; R&D Systems, Minneapolis, MN, USA; #MAB2909-R&D Systems), OPN (goat anti-OPN; #O7635-Sigma-Aldrich), and TRAP (goat anti-TRAP; Santa Cruz Biotechnology, Santa Cruz, CA, USA; #sc-30832-Santa Cruz). After 2 hours of incubation at room temperature, biotinylated secondary antibodies (anti-rat #BA4001, and anti-goat; Vector Laboratories, Burlingame, CA, USA; #BA5000-Vector Labs), and anti-goat N-Histofine Simple Stain Max PO-(Nichirei Biosciences, Tokyo, Japan), were used in PBS and incubated for 30 min at room temperature, followed by several washes with PBS, ABC complex incubation for 30 min, and DAB reaction (ImmPACT DAB; Vector Laboratories) according to manufactured instructions. Counterstaining was performed using Mayer Hematoxylin.

The immunohistochemistry (IHC) quantification was blindly analyzed according to different cohorts. The number of strong positive intensities of each staining was measured using Aperio Image Scope v. 12.3.3 (Leica Biosystems, Buffalo Grove, IL, USA) based on the image pixels to reduce or eliminate human bias. The number of $TNAP^+$ osteoblasts and OPN^+ osteoblasts/osteocytes were also quantified. All osteoblasts located within the osteoid, exhibiting elongated nuclear profiles or tall columnar profiles adjacent to the osteoid, were considered positive. $TRAP^+$ osteoclasts were quantified manually by cell counting in the ossification zone and their adjacent area. All bone cells were quantified at magnification ×20× using ImageJ software.

Primary osteoblasts isolation

Calvariae from 7-day-old 5-LO KO and WT mice were collected, washed with Hank's balanced salt solution (HBSS), and digested in 2.5 mg/mL of collagenase and 1 mg/mL of trypsin solution three times under the water bath shaker at 37°C. The supernatant for the first 15 min of digestion was discarded. The second and third digestions were performed for 30 and 45 min, respectively. The supernatants were transferred to new falcon tubes followed by centrifugation at 364 *g* at room temperature (RT) for 5 min. The pellets were resuspended in a complete culture medium, minimum essential medium (MEM) alpha supplemented with 10% of fetal bovine serum (FBS) plus 1% of penicillin and streptomycin and added in culture flasks. The cells were placed in a CO_2 incubator for the subsequent experiments.[29]

Experimental setup and treatment conditions

For osteoblasts experiments, the cells were plated at densities of 2×10^3, 5×10^3, 2×10^4, 3×10^5, and 1×10^6 cells/well to perform proliferation assay, intracellular calcium (96-well plate), alkaline phosphatase (ALP)/mineralization (24-well plate), quantitative PCR (qPCR)/cyclic adenosine monophosphate (cAMP) (6-well plate), and the proteomic analysis/quantification of eicosanoids (90-mm Petri dishes), respectively. After 48 hours of adhesion, the cells were treated with osteogenic medium (OM) (MEMα plus 10% FBS, 1% antibiotic, and supplemented with 50 μg/mL of ascorbic acid and 10mM β-glycerophosphate). Then the osteoblasts were treated or not (control) with LTB_4 and LTD_4 at 1×10^{-8}M,[24] LTs inhibitors such as MK 886 and MK 591 at 1×10^{-6}M, LTB_4 antagonists such as CP-105696 at 1×10^{-6}M, and U75302 at the dose of 1×10^{-7}M, and CysLTs antagonist MK 571 at 1×10^{-6}M[30,31] up to 21 days. In the control group, the cells were incubated with the same percentage of the vehicle (dimethylsulfoxide [DMSO] or ethanol). The culture medium was changed every 3 days.

Alkaline phosphatase activity

Protein extract from the cell lysate was obtained by adding 200 μL of the buffer containing 10mM Tris (pH 7.5), 0.5mM $MgCl_2$, and 0.1% Triton X-100. ALP activity was given by the conversion of p-nitrophenyl phosphate (pNPP) into p-nitrophenol. Then, the reaction solution (25mM glycine buffer [pH 9.4], 2mM $MgCl_2$, and 1mM pNPP) was added to a 96-well plate and incubated for 30 min at 37°C. Thereafter, 50 μL of the sample (dilution 1:1) was added. The plate was held at 37°C for 30 min. The reaction was quenched with 1M NaOH and the final product was quantified at 405 nm. The results were expressed as ALP activity in nmol of p-nitrophenol $\times$ min^{-1} $\times$ mg^{-1} of protein.[32]

Mineralization assay

The mineralization was evaluated by Alizarin red staining. After 14 and 21 days of culture, the cells were fixed with 10% formalin for 10 min at RT. Then, the cells were incubated with 2% Alizarin solution pH 4.2 for 10 min at RT followed by three washes with ultrapure H_2O. The plates were imaged by using the Kodak Gel Logic 100 Imaging System (Kodak, Rochester, NY, USA). The quantitative analysis was evaluated by the colorimetric method according to da Silva and colleagues.[33] After the plates were completely dry, 280 μL of 10% acetic acid was added directly into each well stained with Alizarin red. The plate was shaken for 30 min at RT. The contents of each well were transferred to microtubes, which were heated at 85°C for 10 min and then kept on ice for 5 min. The tubes were centrifuged at 9.200 *g* for 15 min and 100 μL of the supernatant from each tube was transferred to a 96-well plate. Subsequently, 40 μL of 10% ammonium hydroxide was added to each well to neutralize the acid. The absorbance was measured in a spectrophotometer at 405 nm.[34]

Reverse transcriptase-qPCR

Osteoblast and osteoclast mRNA was isolated by the column extraction method using the RNeasy mini kit (QIAGEN, Valencia, CA, USA; #74106; DNase #79254) according to the manufacturer's instructions. The pellet of the samples was resuspended in 30 μL of diethyl pyrocarbonate (DEPC) water and quantified in Nanodrop (Nanodrop Technologies, Wilmington, DE, USA). Two micrograms of RNA were reverse transcribed and 0.1 μg was used for qPCR reactions. The reverse transcriptase (RT)-qPCR was performed using the Sensi mix Hi-Rox SYBR Green (Bioline, Memphis, TN, USA). The results were expressed as an increased fold in qPCR and normalized by the constitutive GAPDH gene. Table S1 shows the primers used for the gene expression of bone formation and resorption markers, as well as inflammatory markers.

Quantification of intracellular calcium

The assay was performed using the Fluo4-NM Calcium Kit (Molecular Probes, Eugene, OR, USA) according to the manufacturer's instructions. The culture medium was removed, and the

osteoblasts were pretreated with 100 µL of 2.5mM probenecid solution. The plate was incubated for 30–45 min at 37°C. Then, LTB_4, LTD_4, or vehicle was added to the specific wells at reading time. The mean fluorescence intensity was evaluated at excitation at 494 and emission at 516 nm.

Quantification of intracellular cAMP

Intracellular cAMP quantification was performed on 5-LO KO and WT osteoblasts treated or not with LTB_4 and LTD_4 at 7 and 14 days. Prior to collection, the cells were incubated with exogenous LTB_4 and LTD_4 at 1×10^{-6}M for 15 min. The supernatants were discarded, and the cells were lysed by incubation with 0.1M HCl (22°C) for 20 min followed by disruption with a cell scraper. cAMP levels were determined by the enzyme-linked immunosorbent assay (ELISA) immunoassay kit according to the manufacturer's instructions (Cayman Chemical Company, Ann Arbor, MI, USA).

Mass spectrometry analysis of eicosanoids

Quantification, extraction, and concentration of eicosanoids

Cells were washed with PBS and a solution was added containing 3µM of calcium ionophore in HBSS containing Ca^+ and Mg^+ for 30 min incubation at 37°C to stimulate the production of LTs. The supernatant was collected and the same proportion (1:1) of methanol was added. Eicosanoids dissolved in the supernatant are separated from other compounds present in the medium according to their chemical and physical properties, separating low-polarity compounds from the highest-polar compounds. Separation by solid-phase extraction[35] depends on the affinity of the analyte of interest dissolved in a liquid (mobile phase) for the solid phase that fills the cartridge (stationary phase). For this, 10 µL of the solution containing the internal standards was added to each sample (10 ng de AA-d8; 5 ng de 6-KetoPGF2dα-d4, LTC_4-d5, LTE_4-d5; 2 ng de 5-hydroxyeicosatetraenoic acid [HETE]-d8, LTB_4-d5, LTD_4-d5, PGF2ad4, prostaglandin E2 [PGE2]-d4, prostaglandin D2 [PGD2]-d4, thromboxane B2 [TXB2]-d4). Samples were shaken and kept on ice. Meanwhile, the solid-phase extraction (SPE) cartridges were activated with 4 mL of methanol and then conditioned with the same volume of water. After that, the samples were applied to the cartridges properly positioned in the extraction tank and the vacuum pump was turned on to help the sample slowly pass through the SPE cartridge. After passing the entire sample through the cartridge, it was washed with 5 mL of ultra-pure water to remove possible interferences that may have been adsorbed on the stationary phase. Cartridges were well-dried with the help of a vacuum. After that, microtubes were fitted to the extraction tank to collect the elution washes containing the lipids. Then, the eicosanoids were eluted with 1 mL of methanol. After that, the samples were concentrated until completely dry, and then the pellet was resuspended in 50 µL of the solution containing methanol and H_2O (7:3). The samples were transferred to the vials and then inserted into the mass spectrometer Nexera X2 TripleTOF 5600+ System (SCIEX, Framingham, MA, USA).

Proteomic analysis

Total proteins of primary osteoblasts, as well as long bones from females 5-LO KO and WT mice, were extracted in lysis solution (Urea 6M, Thiourea 2M, Dithiothreitol [DTT] 10mM, Ambic 50mM, and Sodium Dodecyl Sulfate 0.1%) at 4°C for 10 min in a shaker, followed by centrifugation at 20.817*g* at 4°C for 10 min, and the supernatant was collected. Long bone samples were macerated in liquid nitrogen prior to their addition to the lysis solution previously described. Total protein quantification was determined by the Bradford Method (1976).[36] After protein quantification, 1 µg/µL was transferred to a microtube, and 10 µL of 50mM AMBIC was added to the sample, followed by 25 µL of *RapiGest SF* 0.2% (Waters Corporation, Milford, MA, USA) and by incubation at 37°C for 60 min. Then, 2.5 µL of 100 mM DTT was added and the samples were homogenized and incubated at 37°C for 40 min. After that, 2.5 µL of 300mM iodoacetamide was added to the samples and incubated for 30 min in RT, in the dark. The proteolytic digestion was performed by 50 ng/µL of trypsin at 37°C overnight and then the enzyme was blocked with 10 µL 5% trifluoracetic acid (TFA) at 37°C for 90 min, and centrifugation of 20.817 *g* at 6°C for 30 min. Peptides were purified and desalinated in *C18 spin* columns, according to the manufacturer. Fifty micrograms of the peptides were dried in a speed vacuum and resuspended in 3% acetonitrile and 0.1% formic acid and, added to a total recovery vial.[37]

Shotgun label-free quantitative proteomic analysis and acquisition of data nano liquid chromatography electrospray ionization tandem mass spectrometry

Data acquisition was performed by Xevo G2 QTof mass spectrometer coupled to the nanoACQUITY Ultra Performance Liquid Chromatography (both from Waters, Manchester, UK) controlled by MassLynx v.4.1 (Waters, Manchester, UK). Data collection was in data-independent acquisition mode ($LC\text{-}MS^E$), the mass ranges from 50 to 2000 m/z, and assays were performed exactly as described.[38,39] All samples were analyzed in biological triplicate and technical triplicate, thus totaling nine analyses for each condition. The proteins were identified using the software's ion counting algorithm, and a search was performed on the *Mus musculus* database (revised only, UniProtKB/Swiss-Prot) downloaded in April 2022 from UniProtKB (http: //www.uniprot.org). Maximum missed cleavages by trypsin allowed up to 1, variable modifications by oxidation, and a false discovery rate value at a maximum of 4%.

For the label-free quantitative analysis, ProteinLynx Global Server (PLGS) version 3.03 (Waters, Manchester, UK) was used for analyzing nine raw MS files from each group. Proteins identified with a confidence score higher than 95% were included. The identical peptides from each duplicate by sample were pooled according to mass accuracy[37] and the retention time tolerance <0.25 min, using the clustering software included in the PLGS. Normalization was automatically implemented by the software (default parameters). The difference in expression between the groups was analyzed by dependent *t*-test ($p < 0.05$). The following relevant comparison was performed: 5-LO KO versus WT osteoblasts.

Bioinformatics analysis

For the in vitro analysis, the proteins were analyzed by their access number by UniProt and repeated proteins, reverse proteins, and fragments were excluded. Gene ontology was evaluated according to the ClueGo® plugins of the Cytoscape® 3.8.2 Software (https://cytoscape.org/). The functional distribution of proteins identified with differential expression in the different

comparisons was done. Protein categories were based on Gene Ontology[35] annotation of the broad Biological Process, Molecular Function, Immune System Process, and Cell Component. Terms of significance (kappa = 0.04) and distribution were according to the percentage of the number of associated genes. The number of accesses to the proteins was provided by UniProt. The mass spectrometry proteomics data have been deposited to the ProteomeXchange Consortium via the PRIDE partner repository with the dataset identifier PXD037911.

For interaction networks of the in vivo analysis, the database STRING® (https://string-db.org/) was used to establish the interaction between proteins identified with differential expression and unique proteins of each group for the comparison of 5-LO KO × WT mice.

Osteoclast isolation

Primary osteoclast precursors from bone marrow were isolated from 7-day-old 5-LO KO and WT mice. Femurs and tibias were triturated in HBSS to release the bone marrow, and the supernatant was centrifuged at 443 *g* for 10 min at RT. The pellet was resuspended in 7 mL of fresh HBSS for cell stratification with histopaque, followed by centrifugation at 560 *g* for 30 min at RT. Monocytes were collected and transferred to a new tube containing 7 mL of HBSS. Centrifugation at 443 *g* for 10 min was done and the pellet was resuspended in 1 mL of complete medium (MEMα plus 10% FBS and 1% antibiotic) and plated in a 3.5-cm Petri dish for 12 min for adhesion of unwanted cells. Cells of the monocytic-macrophagic lineage were maintained with supplementation of the cytokines macrophage colony-stimulating factor (M-CSF) and receptor activator of nuclear factor kappa-B ligand (RANKL).[40]

Experimental design and treatment of cells with cytokines

For the osteoclastogenesis experiments, 4×10^5 cells/well were plated for immunostaining with TRAP and bone resorption assay, in 96-well plates, and 2×10^6 cells/well for qPCR, in 6-well plates. Cells were plated with MEMα culture medium with 10% FBS, 1% penicillin/streptomycin, and supplemented with M-CSF at a concentration of 50 ng/mL. After 3 days, the medium was changed, and RANKL was added at a concentration of 120 ng/mL. The culture medium was changed every 3 days, and the experiment was evaluated for up to 11 days.

Collection and preparation of conditioned medium

Primary murine osteoblasts from 5-LO KO and WT mice were cultured in an OM and the supernatants were collected at 14 days, centrifuged at 393 *g* for 10 min at 4°C, transferred to a new tube, and stored at −80°C for further osteoclastogenic assays. For the experiments, conditioned medium (CM) was used in a ratio of 1:1; ie, 50% of CM and 50% of fresh OM.

TRAP assay

To perform the TRAP assay, primary cells of the monocytic-macrophagic lineage were fixed with 10% formalin for 10 min at RT and then washed with PBS. After that, 100 µL of the solution containing sodium nitrate, fast garnet, Naaptol phosphoric acid solution, acetate, tartrate, and deionized water was added, according to the manufacturer's instructions (Sigma-Aldrich; #387A). The plates were coated with aluminum foil to protect them from light and incubated at 37°C for 60 min at RT. Then, the cells were washed with deionized water and kept dry for image acquisition under an inverted microscope.[40]

Bone resorption assay

Cells of the monocytic-macrophagic lineage were cultured in 96-well plates on bone slices and maintained for up to 11 days with supplementation of 50 ng/mL of M-CSF and 120 ng/mL of RANKL. After the experimental period, the bone slices were washed with PBS buffer solution. Then, the cells were vigorously removed with a cotton swab, rubbing it on the surface of the bone slide, thus removing the adhered cells. After removing the osteoclasts, the bone slides were transferred to the tube, then washed with water, and then stained with 1% toluidine blue dye in water (pH 4.5), shaking the tube for 30 s. Bone slices were rinsed three times with deionized water and after that, the samples were dried with absorbent paper. Afterward, the bone slices were transferred to a glass slide for image acquisition under an optical microscope.[40]

Results

Characterization of the bone phenotype in 5-LO–deficient mice

µCT (Fig. 1*A*,*C–M*) and histological analysis (Fig. 1*B*) revealed the bone profile of mice lacking 5-LO. µCT analysis of femurs in female and male 5-LO KO mice showed increased TV (Fig. 1*C*), TV of the medullary area (Fig. 1*F*), and volume density of the medullary region (Fig. 1*G*). The cortical bone parameters showed increased BV/TV (Fig. 1*D*) and no differences were found in the TV of cortical bone between 5-LO KO and WT mice (Fig. 1*E*). The BV of trabecular bone and the BS/TV was not statistically significant in 5-LO KO related to WT mice (Fig. 1*H*,*J*). Trabecular bone volume (BV/TV), trabecular number (Tb.N), and trabecular thickness (Tb.Th) were decreased in female 5-LO KO but not in male 5-LO KO when compared to WT mice (Fig. 1*I*,*K*,*L*). In addition, the trabecular separation (Tb.Sp) was increased in female and male 5-LO KO mice when compared to WT mice (Fig. 1*M*). In summary, 5-LO absence increases the cortical bone and medullary region in both females and males and decreases trabecular bone in females, but not males.

Bone parameters and hematoxylin and eosin (H&E) staining of the fifth lumbar vertebra were evaluated (Fig. 2*A–K*). µCT analysis of female 5 LO-KO showed less BV, BV/TV (Fig. 2*D*,*E*), and increased BS/TV and BS/BV, when compared to female WT mice (Fig. 2*G*,*H*). TV and BS from both 5-LO KO and WT females was similar (Fig. 2*C*,*F*). Trabecular number (Tb.N) and trabecular separation (Tb.Sp) in female 5-LO KO was higher (Fig. 2*I*,*K*), and trabecular thickness (Tb.Th) was lower when compared to the control WT (Fig. 2*J*).

Localization of TNAP, OPN, and TRAP by immunohistochemistry analysis revealed higher expression and number of $TNAP^+$ osteoblasts in both female and male 5-LO KO mice (Fig. 3*A*,*C*,*F*). Higher levels of OPN but not statistically significant OPN^+ osteoblasts/osteocytes number in 5-LO KO females was observed, whereas males presented higher expression and a higher number of OPN^+ cells (Fig. 3*A*,*D*,*G*). Lower expression and number of $TRAP^+$ osteoclasts in 5-LO KO femurs were seen when compared to WT mice (Fig. 3*B*,*E*,*H*). This result was confirmed by

immunofluorescence quantitative analysis of OPN and TRAP of the femur's growth plate (Fig. S1*A–F*). OPN levels in femurs were higher in both female and male 5-LO KO mice when compared to WT mice (Fig. S1*E*). The expression of TRAP was lower in female and male 5-LO KO in comparison to WT mice (Fig. S1*F*).

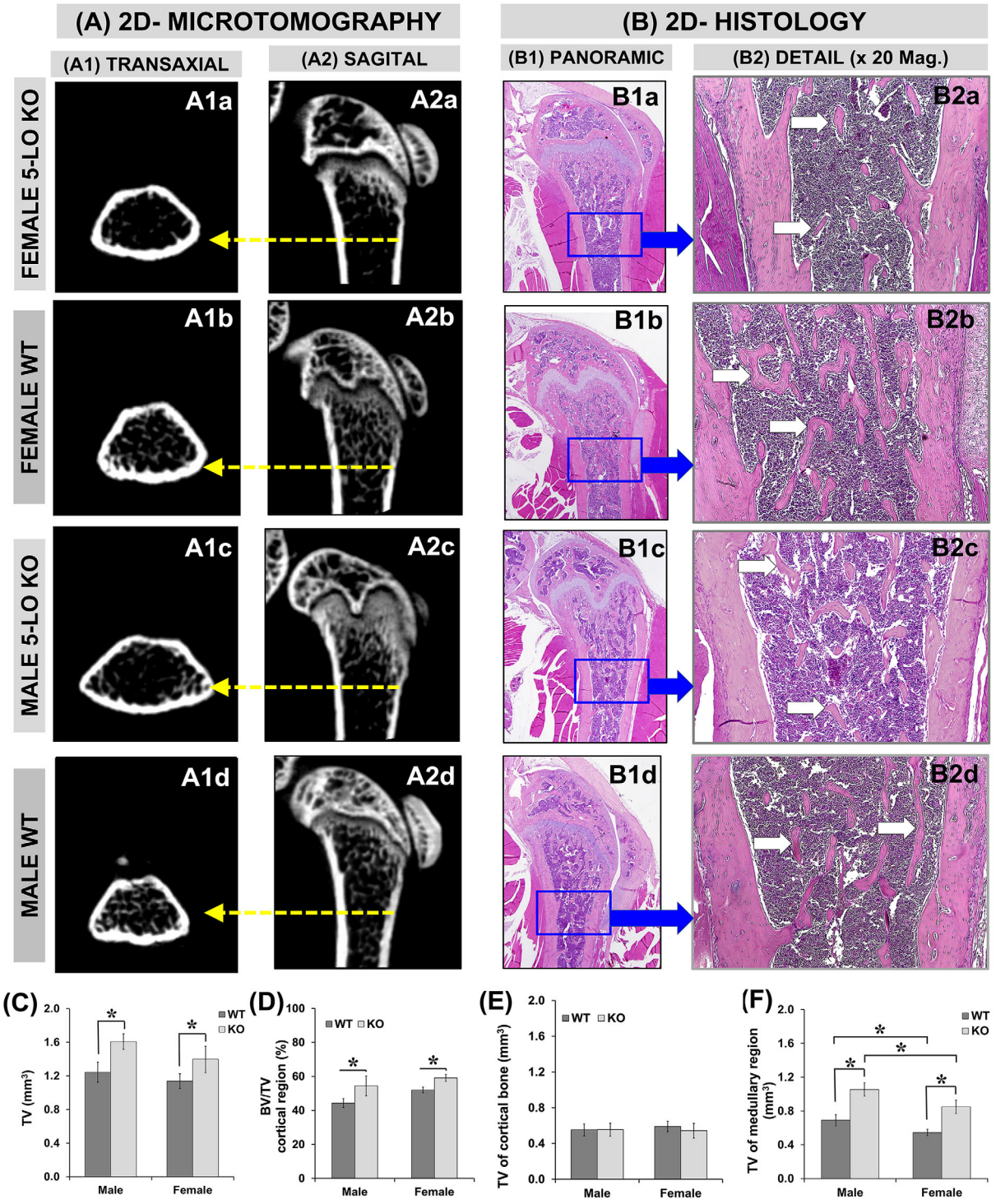

Fig. 1. µCT analysis and H&E staining of the femur from 5-LO KO and WT mice. (*A*) 2D µCT images and (*B*) H&E staining of femurs from 8-week-old females ($n = 10$) and males ($n = 10$) of 5-LO KO and WT mice. µCT analysis of bone parameters in the femurs shows (*C*) tissue volume (TV), (*D*) cortical bone volume fraction (Ct.BV/TV), (*E*) TV of cortical bone (Ct.TV), (*F*) TV of the medullary area, (*G*) volume density of the medullary region, (*H*) bone volume (BV) of trabecular bone, (*I*) Trabecular bone volume (BV/TV), (*J*) bone surface area per total volume (BS/TV), (*K*) trabecular number (Tb.N), (*L*) trabecular thickness (Tb.Th), and (*M*) trabecular separation (Tb.Sp). Statistical analysis was performed by one-way ANOVA followed by Tukey's multiple comparison test. Differences were statistically significant at $^*p < 0.05$.

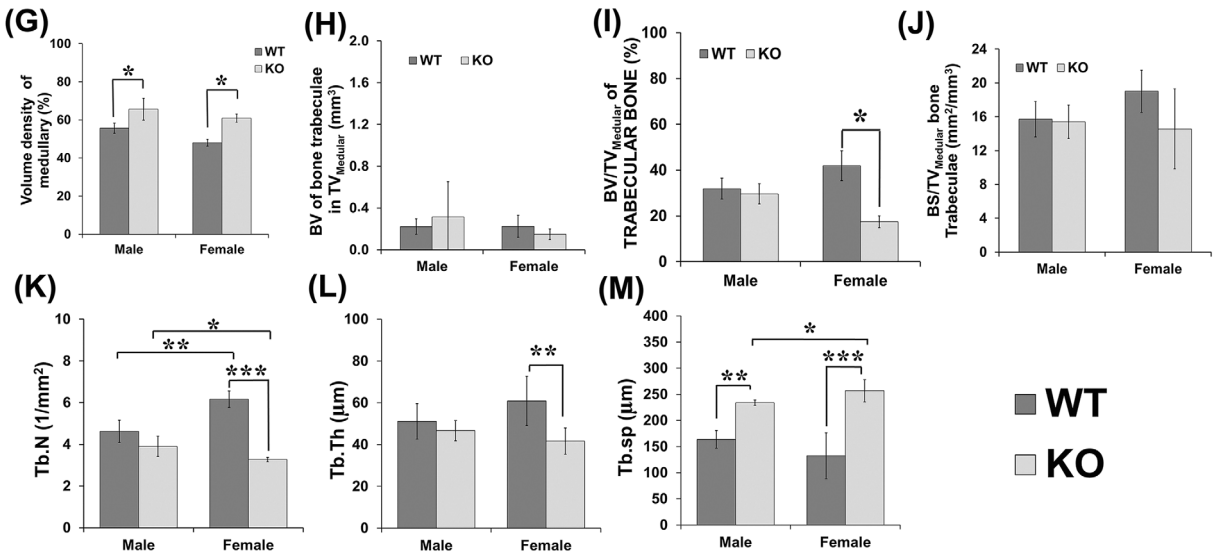

Fig. 1 (Continued)

5-LO absence decreases the proliferation and enhances osteoblasts differentiation and mineralization in vitro

We examined the role of endogenous leukotrienes on osteoblast proliferation, differentiation, and mineralization. Primary osteoblasts isolated from WT and 5-LO KO mice calvaria were cultured in an OM and an 3-(4,5-dimethylthiazol-2yl)-2,5-diphenyltetrazolium bromide (MTT) proliferation assay was performed on days 1, 2, and 4 of osteoblast culture. The results showed the osteoblast proliferation rate was significantly decreased at all three time points in the 5-LO KO compared to the WT mice, $p < 0.001$ (Fig. 4*A*). Additionally, we performed flow cytometry–carboxyfluorescein succinimidyl ester (CFSE)-based cell proliferation assay on days 2 and 4 of WT and 5-LO KO osteoblast culture, and the results showed osteoblast proliferation was lower on days 2 and 4 of 5-LO KO compared to the WT osteoblasts (Fig. 4*B*).

The ALP activity assay was performed on days 4, 7, 10, and 14 of primary osteoblasts collected from WT and 5-LO KO mice calvaria and cultured in an OM. Results showed ALP activity is higher in all four time points of osteoblasts cultured from 5-LO KO compared to the WT mice (Fig. 4*C*).

Additionally, we studied the effect of 5-LO and LTs on osteoblast mineralization. Thus, osteoblasts from WT and 5-LO KO mice were cultured for 14 and 21 days in an OM, and Alizarin red staining was performed. Results showed the mineralization rate was higher in 5-LO KO compared to WT mice, in both time points (Fig. 4*D*). Also, we cultured primary osteoblasts from 5-LO KO mice in an OM with exogenous leukotrienes such as LTB_4 and LTD_4 for 21 days and performed a mineralization assay and the results showed both, LTB_4 and LTD_4 treatment significantly decreased the mineralization in 5-LO KO when compared to untreated 5-LO KO cells, and that LTB_4 was more effective in reducing the mineralization than LTD_4 (Fig. 4*E*).

Furthermore, osteoblasts from WT mice were cultured in an OM for 21 days with exogenous leukotrienes such as LTB_4 and LTD_4 and their inhibitors, MK886 and MK591, respectively. Also, LTB_4 receptor antagonists were used such as CP-105696 and U75302, and the combination of U75302 + exogenous LTB_4, LTD_4 receptor antagonist MK571, and MK571 + exogenous LTD_4. Mineralization assay results showed exogenous LTB_4 and LTD_4 treatments significantly decreased the mineralization compared to the untreated osteoblasts, whereas the LT inhibitors MK886 and MK591 treatments, and the LTB_4 antagonists CP-105696, and U75302 increased the mineralization, and U75302 + exogenous LTB_4 treatment did not show increased mineralization. Neither MK571 treatment nor MK571 + exogenous LTD_4 increased the mineralization when compared to untreated cells (Fig. S2).

Gene expression of Alox5 (gene encoding 5-LO) and osteogenic markers was performed by qPCR. Results demonstrated that Alox5 is highly expressed during the differentiation of WT osteoblasts, within 10 and 14 days of culture when compared to day 0. Even though Alox5 had a higher expression on days 10 and 14 of osteoblast differentiation, there were detectable levels of Alox5 expression on all studied time points (Fig. 5*A*). Alkaline phosphatase (Alpl) gene expression in the WT and 5-LO KO mice osteoblasts from 0 up to 14 days of culture showed increased Alpl in all time points in 5-LO KO compared to WT osteoblasts culture (Fig. 5*B*). The transcription factors Runt-related transcription factor 2 (Runx2) and Sp7, also called Osterix,[41] were slightly modulated in 5-LO KO osteoblasts, showing downregulation of Runx2 within 2 days and upregulation of Sp7 within 7 and 14 days of culture, compared to WT osteoblasts (Fig. 5*C*,*D*). Results from qPCR analysis of Bglap showed osteocalcin messenger RNA (mRNA) expression was higher in early time points (days 0, 2, and 4), and later time points (days 10 and 14) of 5-LO KO compared to WT osteoblasts (Fig. 5*E*). Tnfsf11 (encoding RANKL) normalized by OPG was overexpressed in 5-LO KO cells at all time points related to the control WT osteoblasts (Fig. 5*F*). The gene expression analysis of the matrix metalloproteinases MMP-2 and MMP-9 showed overexpression in 5-LO KO mice osteoblasts on 0, 7, and 14 days for MMP-2, and 4 and 7 days for the MMP-9 gene when compared to WT osteoblasts (Fig. 5*G*,*H*). Most of the osteogenic factor expression was upregulated in 5-LO KO mice in almost all the time points of osteoblasts differentiation despite Alox5 expression being higher only on the 10th and 14th days of osteoblast differentiation. These results demonstrated that LTs affect osteoblastic gene expression in a

complex manner. Taken together, these results indicate the possible paracrine actions of endogenous leukotrienes on osteoblasts. We demonstrated that the absence of 5-LO decreased the proliferation and increased osteoblast differentiation and mineralization, indicating the antagonist role of endogenous LTs signaling in osteoblast-mediated bone formation.

Also, we evaluated the regulation of exogenous LTB_4 and its antagonist U75302 by qPCR analysis for collagen type 1a

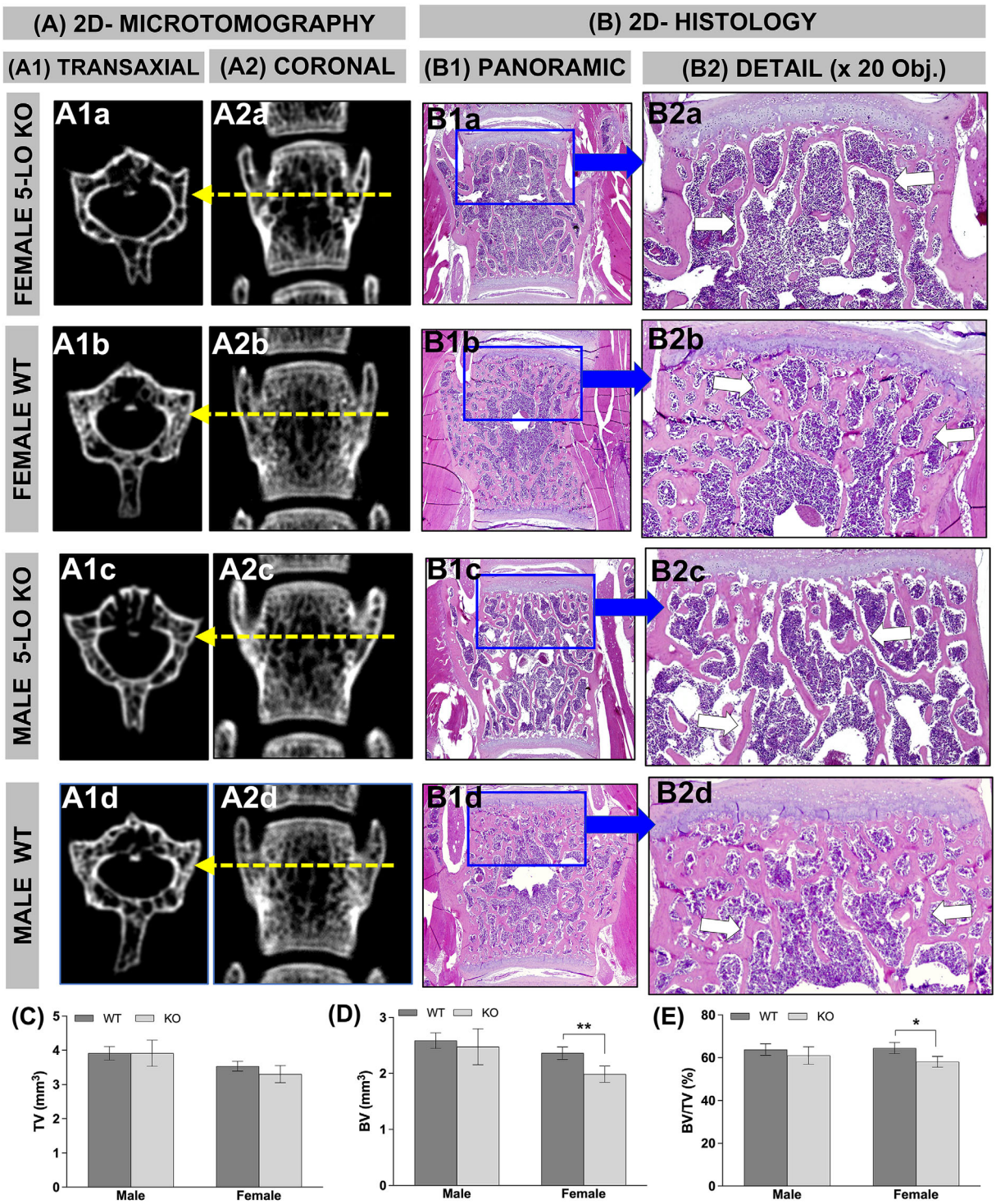

Fig. 2. µCT analysis and H&E staining of the vertebra from 5-LO KO and WT mice. (*A*) 2D µCT images and (*B*) H&E staining of vertebrae from 8-week-old females and males of 5-LO KO and WT mice. Bone parameters of the fifth lumbar vertebra: (*C*) tissue volume (TV), (*D*) bone volume (BV), (*E*) trabecular bone volume (BV/TV), (*F*) trabecular bone surface (BS), (*G*) bone surface area per total volume (BS/TV), (*H*) bone surface per bone volume (BS/BV), (*I*) trabecular number (Tb.N), (*J*) trabecular thickness (Tb.Th), (*K*) trabecular separation (Tb.Sp). Statistical analysis was performed by one-way ANOVA followed by Tukey's multiple comparison test. Differences were statistically significant at $*p < 0.05$.

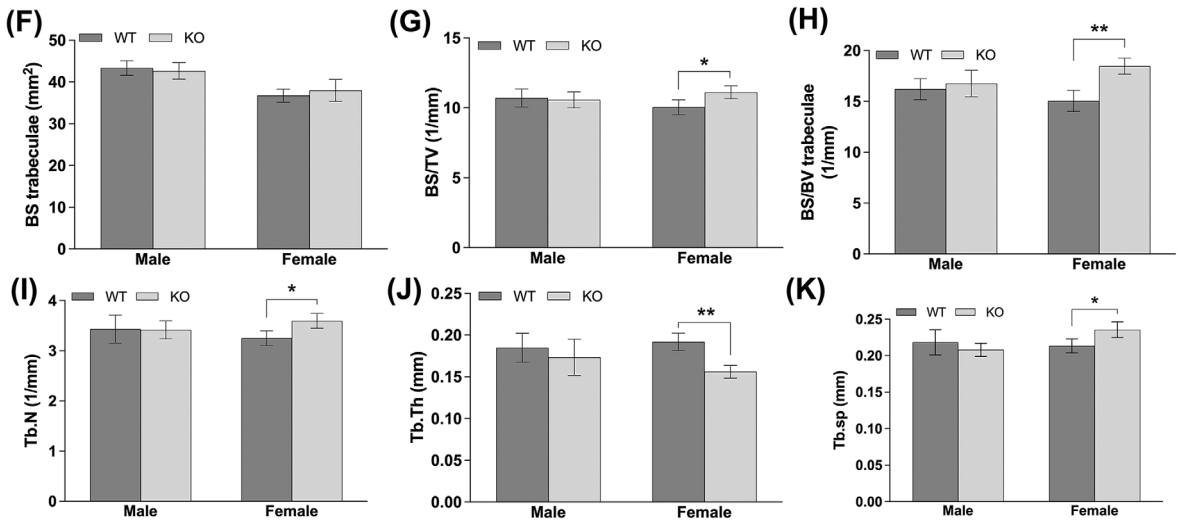

Fig. 2 (Continued)

(Cola1a), Runx2, Sp7, Tnfsf11, MMP-2, and MMP-9 from 5-LO KO and WT osteoblasts. Collagen 1a expression was decreased in the 5-LO KO osteoblasts compared to WT osteoblasts cultured for 4 days. The treatment with LTB_4 or U75302 did not modulate the Cola1a expression. Collagen 1a expression was lower in 14 days of osteoblast culture and there were no differences between 5-LO KO and WT cells nor the treated group (Fig. S3*A*). Runx2 expression was higher only in U75302-treated 4 days cultured WT osteoblasts compared to all other treatments. At 14 days of culture, Runx2 expression was downregulated by the exogenous LTB_4 treatment in WT cells and U75302 increased Runx2 expression in osteoblasts from 5-LO KO compared to LTB_4 treated 5-LO KO osteoblasts. Runx2 expression was decreased in 5-LO KO cells treated with U75302 antagonist within 4 days but increased after 14 days of culture when compared to WT cells (Fig. S3*B*).

Results showed early osteoblasts marker Sp7 expression was higher in 4 days of culture from 5-LO KO osteoblasts compared to WT osteoblasts. The treatment with LTB_4 downregulated the Sp7 expression in 5-LO KO osteoblasts but not in WT cells. LTB_4 receptor antagonist U75302 rescued the effect in 5-LO KO cells. At 14 days of osteoblast culture, Sp7 expression was almost undetectable in cells of any of the treatments (Fig. S3*C*). Tnfsf11 expression was higher in 5-LO KO osteoblasts than WT cells and, LTB_4 treatment downregulated the Tnfsf11 expression in 5-LO KO cells at 4 and 14 days of culture. Exogenous LTB_4 treatment overexpressed Tnfsf11 in WT cells within 14 days (Fig. S3*D*). MMP2 expression was not modulated in osteoblasts cultured for 4 days, whereas it was increased in the 5-LO KO osteoblasts in relation to WT osteoblasts cultured for 14 days (Fig. S3*E*). The MMP-9 expression in 5-LO KO osteoblasts was higher at 4 days but lower within 14 days when compared to WT cells. LTB_4 and U75302 treatments did not modulate the MMP-9 gene expression (Fig. S3*F*). Results demonstrated that LTs affect osteoblastic gene expression in a complex manner.

Effects of endogenous and exogenous LTs on second messengers in osteoblastogenesis

We examined intracellular calcium ($_i Ca^{2+}$) and cAMP levels in osteoblasts. We cultured osteoblasts from 5-LO KO and WT mice for 7 days and 14 days under an osteogenic culture medium with or without exogenous LTB_4 and LTD_4. Results demonstrated that intracellular calcium levels were higher in 5-LO KO osteoblasts compared to WT osteoblasts cultured for 7 days and 14 days. Intracellular calcium levels were lower in LTB_4-treated 5-LO KO and WT osteoblasts related to untreated cells, and lower in LTD_4-treated 5-LO KO cells when compared to untreated 5-LO KO cells within 14 days of culture (Fig. S4*A*).

Results demonstrated that cAMP was not regulated in 5-LO KO and WT osteoblasts cultured for 7 days, whereas at day 14, the intracellular cAMP levels were decreased in 5-LO KO osteoblasts when compared to WT osteoblasts. The exogenous LTB_4 and LTD_4 treatment did not modulate both 5-LO KO and WT osteoblasts. cAMP levels were lower in LTD4-treated 5-LO KO cells than in LTB_4-treated 5-LO KO osteoblasts (Fig. S4*B*).

5-LO absence affects eicosanoids production in osteoblasts

The eicosanoid quantification in 5-LO KO and WT osteoblasts was examined by mass spectrometry (Table S2). Cells from 5-LO KO and WT mice were cultured for 7 days and 14 days in the OM and the production of the eicosanoids in osteoblasts was measured. Results demonstrated that the 11-HETE level was higher in 7 days and 14 days of cultured 5-LO KO osteoblasts compared to WT osteoblasts (Fig. 6*A*). The 15-HETE level was undetectable in 7 days in WT osteoblasts but it was highly expressed in 7 days in 5-LO KO osteoblasts, and it was higher in 14 days of culture of 5-LO KO osteoblasts compared to 14 days of WT osteoblasts (Fig. 6*B*). 15-Keto-PGE2 production was higher in 5-LO KO osteoblasts than in WT cells in both periods. The 15-keto-PGE2 level was undetectable at 7 days and 14 days in WT osteoblasts (Fig. 6*C*).

6-Keto-PGF1a level was not modulated in 7 days in 5-LO KO and WT osteoblasts but it was higher at 14 days of cultured 5-LO KO osteoblasts when compared to 14 days of WT osteoblasts (Fig. 6*D*). The AA level was higher in cultured 5-LO KO osteoblasts at 7 days than in 14 days of WT osteoblasts and it was not modulated in 14 days of culture (Fig. 6*E*). Eicosapentaenoic acid

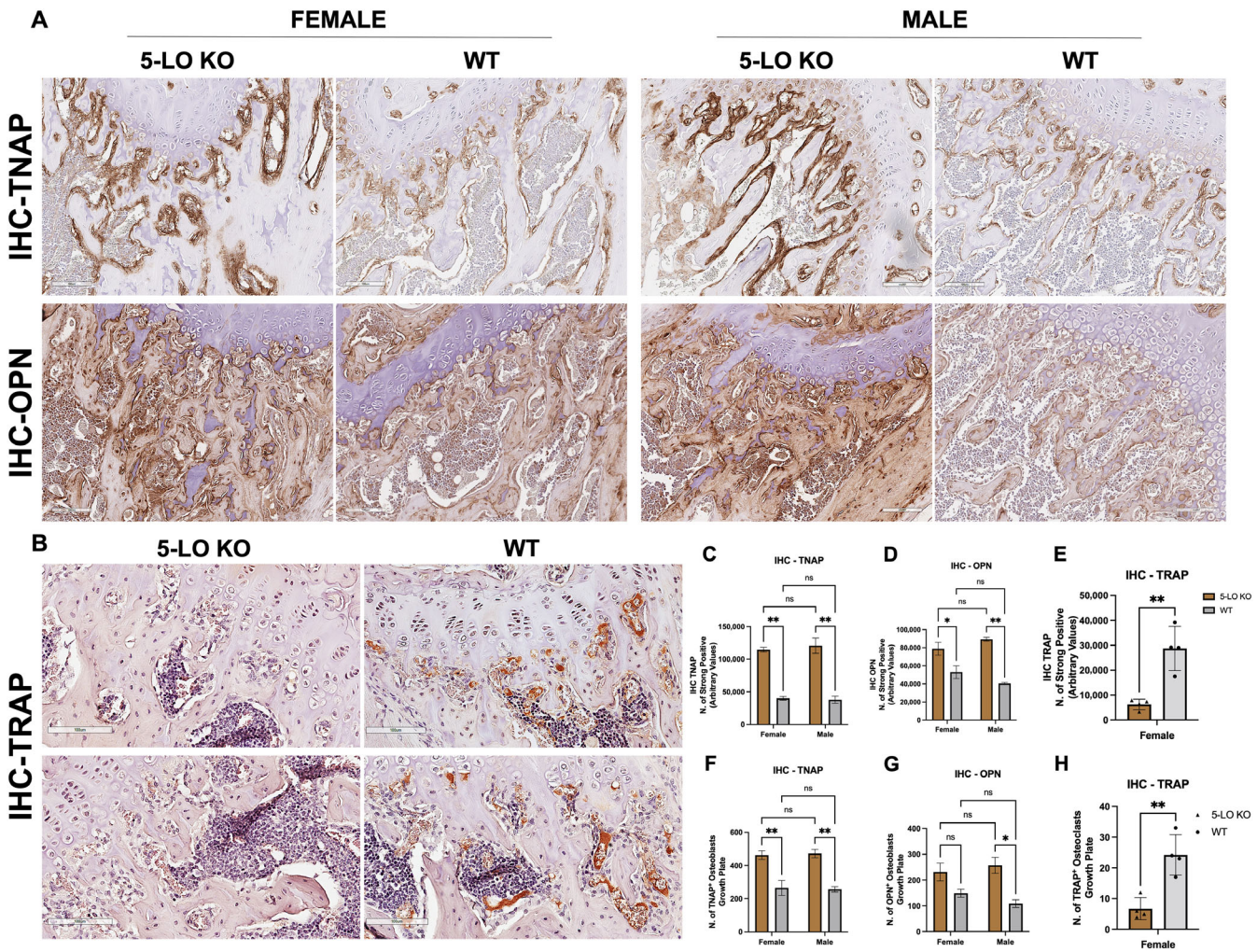

Fig. 3. Visualization of tissue nonspecific alkaline phosphatase (TNAP), osteopontin (OPN), and tartrate-resistant acid phosphatase (TRAP) in femurs of 5-LO KO and WT mice by immunohistochemistry. (*A*) TNAP and OPN IHC show higher expression and (*B*) TRAP IHC shows impaired expression in 5-LO KO versus WT mice. Counterstaining was performed using Mayer Hematoxylin. Scanning of the tissue sections was done by the Aperio AT2 system (Leica Biosystems of Leica Microsystems Inc., Buffalo Grove, IL, USA). (*C–E*) Immunohistochemistry (IHC) quantification for TNAP, OPN, and TRAP shown as the number of strong positive staining intensity, measured using Aperio Image Scope v. 12.3.3 (Leica Biosystems). (*F–H*) Represents quantification of the number of $TNAP^+$ osteoblasts, OPN^+ osteoblasts/osteocytes, and $TRAP^+$ osteoclasts, respectively, in the femur's growth plate of 5-LO KO versus WT mice at magnification ×20 using ImageJ software (National Institutes of Health, NIH, Bethesda, MD, USA).

(EPA) production was higher in 7 days and 14 days of cultured 5-LO KO osteoblasts compared to WT osteoblasts (Fig. 6*F*). LTB_4 production in WT osteoblasts was higher in 14 days when compared to 7 days of culture. The level of LTB_4 in 5-LO KO osteoblasts was undetectable (Fig. 6*G*). Prostaglandins PGA_2, PGB_2, PGE_2, and PGF2a levels were not modulated in 7 days but they were higher in 14 days in 5-LO KO osteoblasts compared to WT osteoblasts (Fig. 6*H–K*). TXB2 level was not modulated in 7 days but it was lower in 14 days of cultured 5-LO KO osteoblasts when compared to WT osteoblasts (Fig. 6*L*).

Proteomic analysis

Fifty micrograms of protein were recovered from 5-LO KO and WT osteoblasts. A total of 124 proteins were identified, considering all groups. In the comparison between 5-LO KO versus WT, the total number of proteins identified was 120 and 81, respectively, among which 77 proteins were common to both groups, such as *Serum albumin* and *Beta-enolase*. Forty-three proteins were identified exclusively in the 5-LO KO, such as *Galectin-1*, *Galectin-3*, *Filamin-A*, *Peroxiredoxin-4*, *Prosaposin*, *Polyubiquitin-B*, *Polyubiquitin-C*, and 20 isoforms of Histone, while four proteins were uniquely identified in the WT, such as *Alpha-internexin*, *Neurofilament heavy polypeptide*, *Neurofilament light polypeptide*, and *Neurofilament medium polypeptide* (Fig. 7*A*, Table S3). In the differentially expressed proteins, only downregulated proteins were identified with 75 proteins decreased in the 5-LO KO osteoblasts. Among the downregulated proteins in 5-LO KO osteoblasts are *Peroxiredoxin-1* (five-fold decreased), *Desmin* (four-fold decreased), *Fibronectin*, *Elongation factor 1-alpha 2*, 12 isoforms of Histone, and Tubulin, among others (Fig. 7*B*, Table S3).

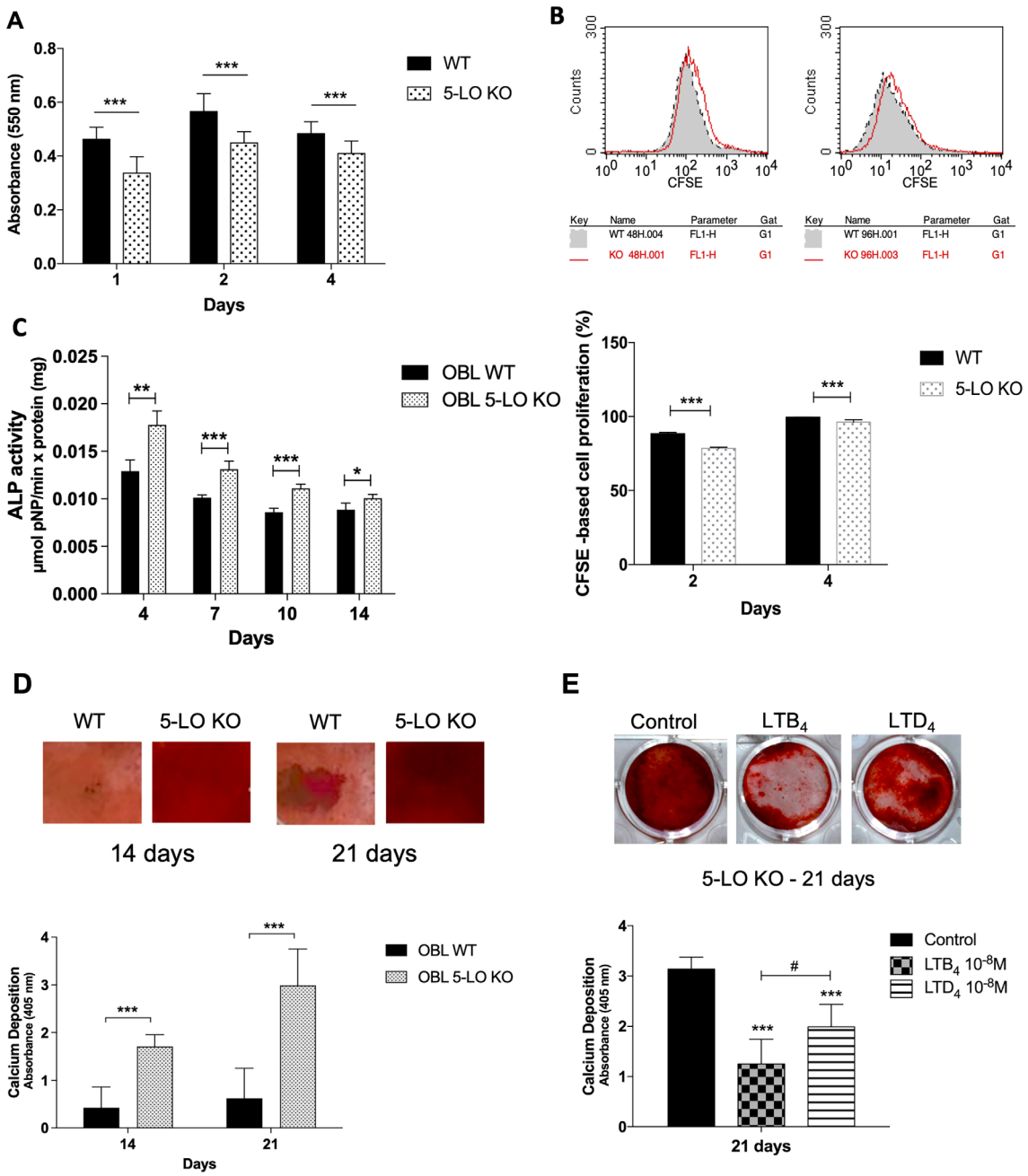

Fig. 4. Effect of leukotrienes on osteoblasts' proliferation, differentiation, and mineralization. Primary osteoblasts from calvaria isolated from 5-LO KO and WT mice were cultured in an osteogenic medium (OM). (*A*) MTT assay was performed on days 1, 2, and 4 of osteoblast culture. Experiments were done in triplicate ($n = 8$/group/experiment). (*B*) Proliferation profile of 5-LO KO and WT osteoblasts by flow cytometry. Cells were labeled with 10µM of CFSE and immediately acquired using the flow cytometer FACS Calibur (BD Biosciences, San Jose, CA, USA). Data were presented as a percentage (%) of cell growth. Results of three independent experiments ($n = 3$/group/experiment). (*C*) Alkaline phosphatase (ALP) activity assay was performed on days 4, 7, 10, and 14. Results represent the mean of the enzyme activity in µmol of para-Nitrophenol (p-NP)/minute by the amount of total protein in mg ± SD. Representation of three independent experiments ($n = 5$/group/experiment). (*D*) Mineralization assay at 14 and 21 days by alizarin red. Images and calcium deposition quantification in the comparison between 5-LO KO versus WT osteoblasts. Triplicates. ($n = 6$/group/experiment). (*E*) Images and quantification of alizarin red staining from osteoblasts treated with exogenous LTB_4 (1×10^{-8}M), LTD_4 (1×10^{-8}M), or vehicle (control). Representation of three independent experiments ($n = 6$ group/experiment). Statistical analysis was performed by unpaired Student's *t* test or by one-way ANOVA followed by Tukey's multiple comparison test (*$p < 0.05$, **$p < 0.01$, ***$p < 0.001$).

In Fig. 7C we show the functional analysis according to the biological process, cellular component, molecular function, and immune system process by Gene Ontologies with the most significant term, for the comparison between 5-LO KO versus WT osteoblasts. Among them, the categories with the most percentages of genes were a *structural constituent of the*

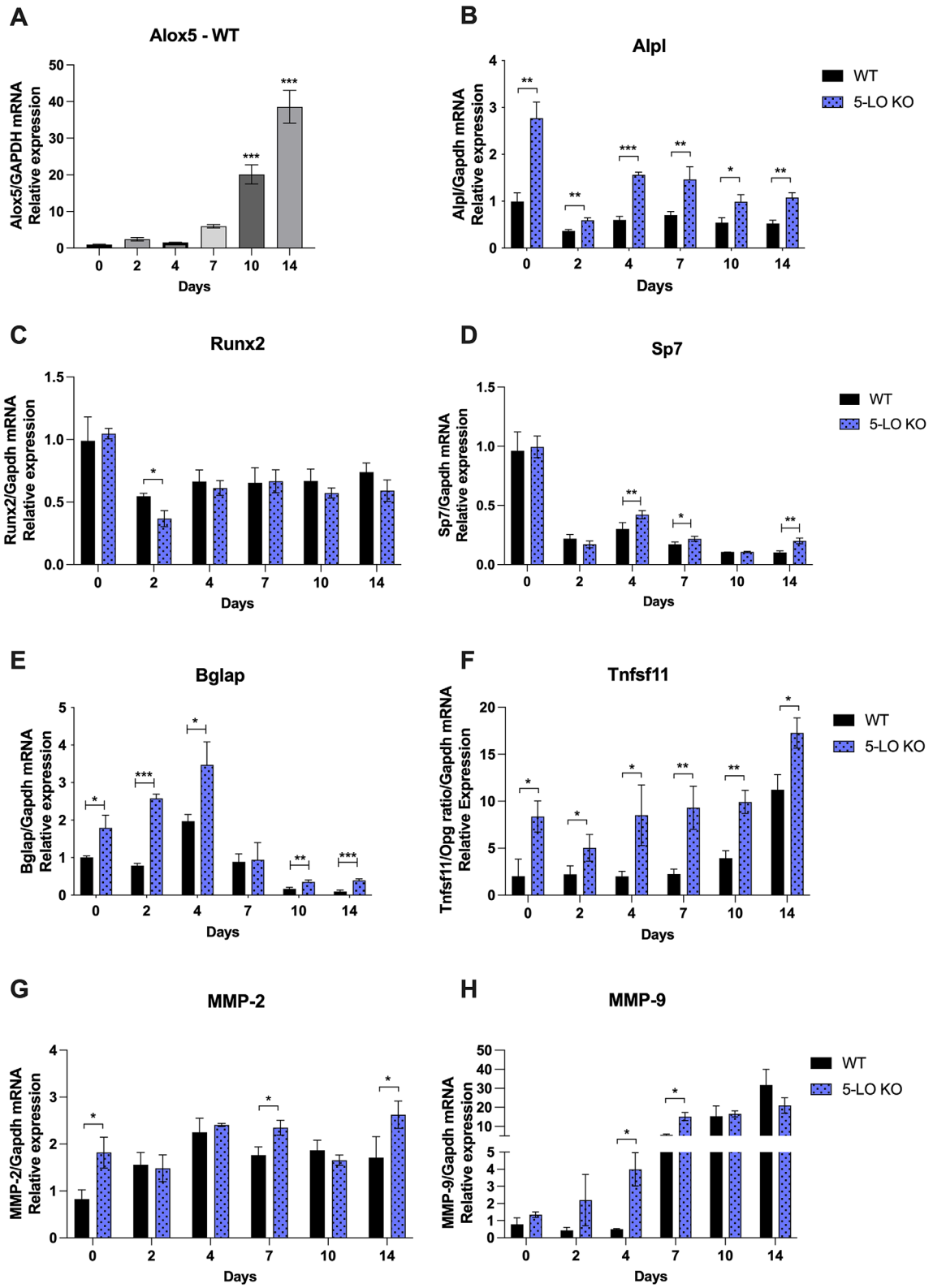

Fig. 5. Gene expression of primary osteoblasts from 5-LO KO and WT animals up to 14 days of culture. (*A*) Alox5, (*B*) Alpl, (*C*) Runx2, (*D*) Sp7, (*E*) Bglap, (*F*) Tnfsf11, (*G*) MMP-2, and (*H*) MMP-9. The data presented are results of the mean, ±SD of three independent experiments ($n = 3$/group/experiment). Statistical analysis was performed by the Unpaired Student's *t* test (*$p < 0.05$, **$p < 0.01$, ***$p < 0.001$).

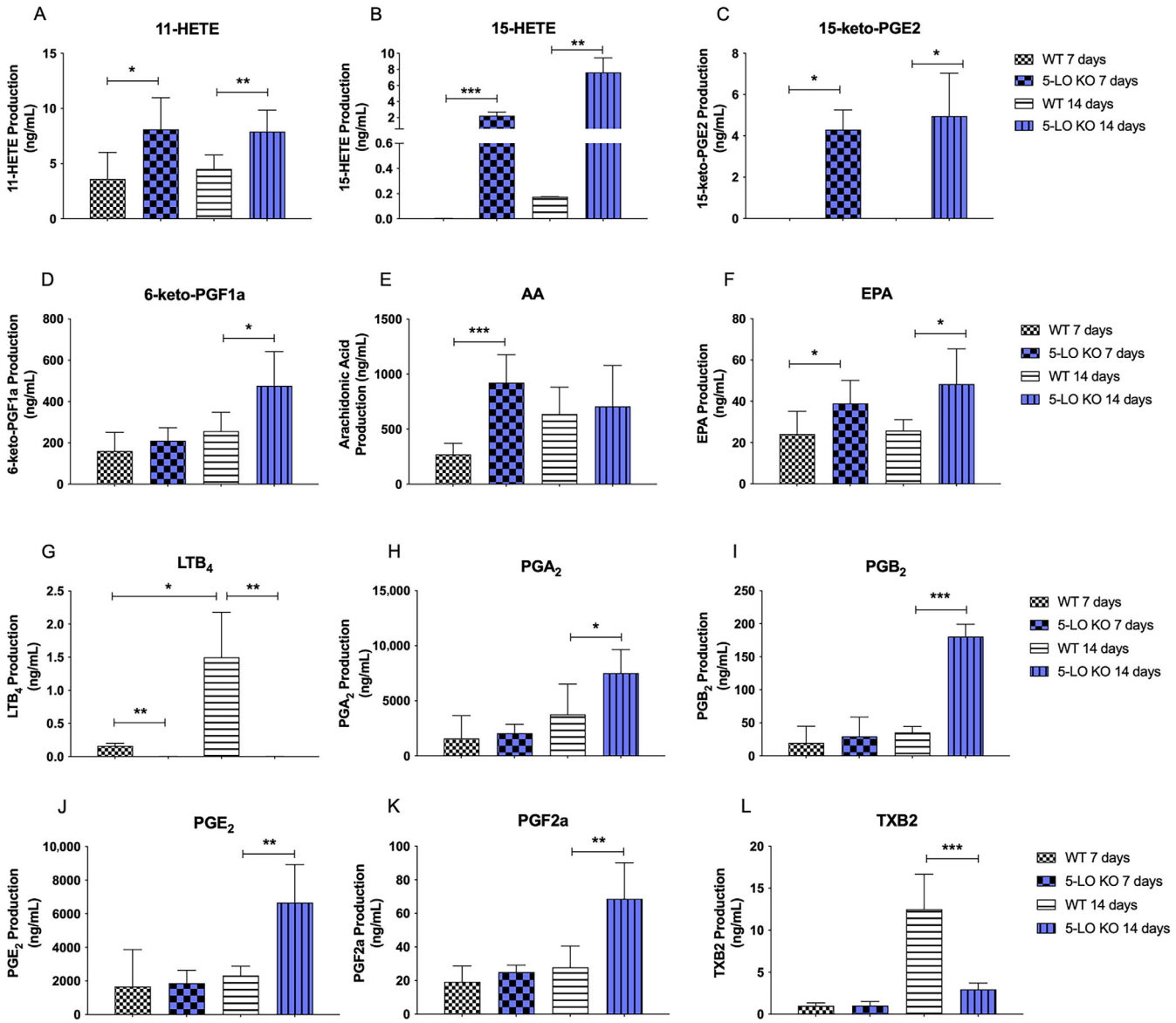

Fig. 6. Quantitative analysis of eicosanoid production in osteoblasts from 5-LO KO and WT mice. Cells were stimulated with 3μM calcium ionophore, and after 7 and 14 days of culture, samples were acquired using a mass spectrometer. Main quantified eicosanoids: (*A*) 11-HETE (11-hydroxyeicosatetraenoic acid); (*B*) 15-HETE (15-hydroxyeicosatetraenoic acid); (*C*) 15-keto PGE2 (15-keto prostaglandin E2); (*D*) 6-Keto PGF 1 α (6-keto prostaglandin F1α); (*E*) AA (arachidonic acid); (*F*) EPA (eicosapentaenoic acid); (*G*) LTB_4 (leukotriene B_4); (*H*) PGA_2 (prostaglandin A_2); (*I*) PGB_2 (prostaglandin B_2); (*J*) PGE_2 (prostaglandin E_2); (*K*) PGF2α (prostaglandin F2α); (*L*) TXB2 (thromboxane B2). Data were presented as the mean ± SD of the values of each eicosanoid in ng/mL from three independent experiments ($n = 6$). Statistical analysis was performed by one-way ANOVA followed by Tukey's multiple comparison test. Differences were statistically significant at $^*p < 0.05$.

cytoskeleton (23.68%), *nucleosome* (68.4%), *major histocompatibility complex (MHC) class I protein binding* (18.75%), and *peptide antigen assembly with MHC class I protein complex* (100%) for biological process, cellular component, molecular function, and immune system process, respectively.

Proteomic analysis of long bones from females 5-LO KO and WT was also performed. A total of 75 proteins were identified, among which eight proteins were common to 5-LO KO and WT groups, such as *AP-1 complex subunit mu-1* and *Protein patched homolog 2*, and they were differentially upregulated and downregulated, respectively, in 5-LO KO long bones. Fifty-six proteins identified were unique to 5-LO KO mice, such as *Carbonic anhydrase 1*, and 19 proteins were exclusive to WT mice, such as the *Interleukin-9 receptor* (Fig. S5*A*, Table S4). Fig. S5*B* shows the interaction networks between upregulated, downregulated, and unique proteins identified in 5-LO KO and WT groups in the in vivo analysis for the following comparison: 5-LO KO versus WT. Results showed functional analysis related to mesenchyme migration, cellular component organization, and muscle cell cellular homeostasis (Fig. S5*B*).

Absence of 5-LO affects osteoclastogenesis

Bone marrow-derived monocytes from 5-LO KO and WT mice were cultured in an osteoclast differentiation medium. After

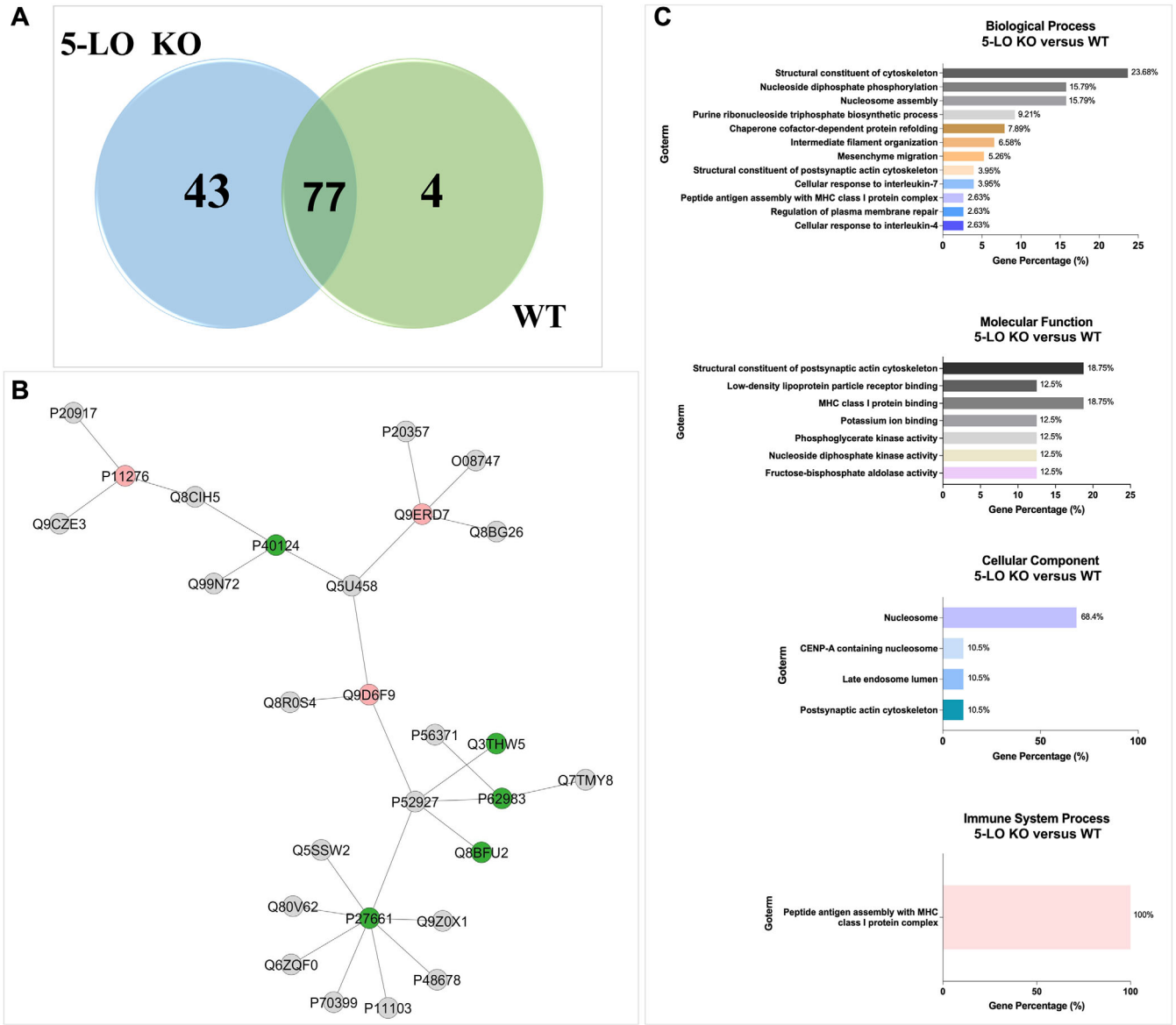

Fig. 7. Functional characterization and network of proteins identified in the proteomic analysis of osteoblasts from 5-LO KO and WT mice after 14 days of culture under an osteogenic medium. (*A*) Venn diagram showing the relation of the proteins identified in common between the groups, as well as the number of proteins identified exclusively in each of the groups. Comparison 5-LO KO versus WT, 43 unique proteins in the 5-LO KO, four unique proteins in the WT, and 77 proteins in common between the groups. (*B*) Subnetworks created by ClusterMarker® to establish the interaction between proteins identified with differential expression in the 5-LO KO osteoblasts versus WT cohort. The color of the nodes indicates the differential expression of the respectively named protein with its access code. The dark green nodes indicate proteins unique to the 5-LO KO osteoblasts. The light red nodes indicate the downregulation of proteins in 5-LO KO osteoblasts. The nodes in gray indicate the interaction proteins that are offered by CYTOSCAPE®, which were not identified in the present study. The identified proteins in this network are described in the supplemental material (Fig. S7). (*C*) Functional analysis of the distribution of proteins identified with differential expression in the 5-LO KO versus WT. Protein categories based on Gene Ontology (GO) annotation of the broad Biological Process, Cell Component, Molecular Function, and Immune System Process. Terms of significance (kappa = 0.04) and distribution according to the percentage of the number of associated genes. The number of accesses to proteins was provided by UniProt. The gene ontology was evaluated according to the ClueGo® plugins of the software Cytoscape® 3.7.2.

11 days of culture, we observed matured osteoclasts only on WT cells but not in 5-LO KO. In fact, different cell phenotypes (clumps of precursors) were observed in 5-LO KO culture (Fig. S6). Next, we cultured monocytes for 11 days from 5-LO KO and WT mice under osteoclast differentiation medium in the presence of the CM from 5-LO KO or WT osteoblasts (cultured for 14 days). TRAP staining and bone resorption assay[42] was performed to calculate mature osteoclasts and TRAP-positive osteoclasts precursors as well as the osteoclast function. Results clearly showed that WT culture presented matured multinucleated osteoclasts and areas of bone resorption (Fig. 8*A*,*D*), whereas 5-LO KO mice

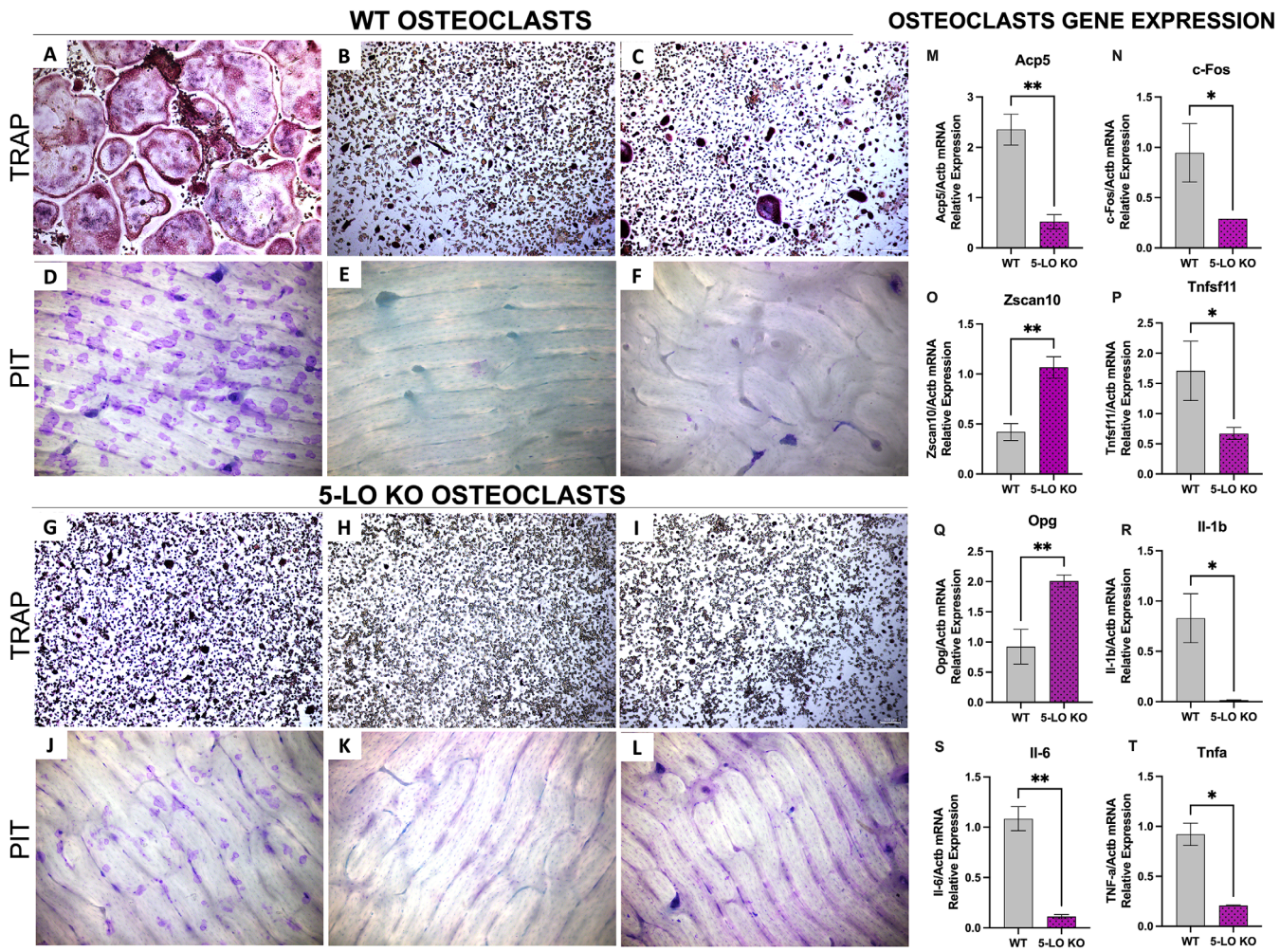

Fig. 8. Effect of endogenous LTs in osteoclastogenesis. Morphology and quantification of TRAP activity, bone resorption assay (PIT), and gene expression in cells derived from the monocytic-macrophage lineage from 5-LO KO and WT mice, after 11 days of culture under stimulation with M-CSF (50 ng/mL) and RANKL (120 ng/mL). (*A–C*) TRAP assay in WT cells, (*A*) untreated or treated with (*B*) conditioned medium from WT or (*C*) 5-LO KO osteoblasts. (*D–F*) PIT assay in WT cells, (*D*) untreated or treated with (*E*) conditioned medium from WT or (*F*) 5-LO KO osteoblasts. (*G–I*) TRAP assay in 5-LO KO cells, (*G*) untreated or treated with (*H*) conditioned medium from WT or (*I*) 5-LO KO osteoblasts. (*J–L*) PIT assay in WT cells, (*J*) untreated or treated with (*K*) conditioned medium from WT or (*L*) 5-LO KO osteoblasts. (*M–T*) Gene expression of bone and inflammatory markers. Statistical analysis was performed by the unpaired Student's *t* test (*$p < 0.05$, **$p < 0.01$, ***$p < 0.001$).

culture hardly had any matured osteoclasts but with the presence of TRAP-positive immature preosteoclasts and impaired bone resorption (Fig. 8*G,J*).

TRAP staining results demonstrated that the treatment with the conditioned medium from 5-LO KO and WT osteoblasts decreased the number of $TRAP^+$ cells and inhibited osteoclast differentiation in both 5-LO KO and WT bone marrow-derived monocytes culture (Fig. S7*A,B*; Fig. 8*B,C,H,I*). The osteoblast-conditioned medium from both 5-LO KO and WT mice impaired bone resorption by osteoclasts (Fig. 8*E,F,K,L*).

Gene expression of osteoclast markers from bone marrow–derived monocytes of 5-LO KO and WT mice after 11 days under osteoclast differentiation medium was evaluated. Results from the comparison between 5-LO KO versus WT cells showed the Acp5, c-Fos, Tnfsf11, IL-1b, IL-6, Tnfa, Tm7sf4, Sost, and BLT1 expression was lower in 5-LO KO cells (Fig. 8*M,N,P,R–T*; Fig. S8*A–C*) and Zscan10, Opg, and Ctsk expression were higher in 5-LO KO cells when compared to WT osteoclasts (Fig. 8*O,Q*; Fig. S8*J*). There were no differences in the gene expression of BLT2 and CysLT1 receptors, Nfatc1, Atf1, Atf2, and Stat3 (Fig. S8*D–I*). In addition, the gene Alox5 was undetectable in 5-LO KO bone marrow–derived monocytes whereas in WT cells it was expressed after 11 days of culture (Fig. S8*K*).

The treatment with exogenous LTB_4 and its receptor antagonist U75302 in the gene expression of bone marrow–derived WT monocytes under osteoclast differentiation medium was evaluated. Results showed that LTB_4 treatment upregulated Acp5, Nfatc1, Ctsk, IL-1b, and IL-6 expression, but not Tnfa when compared to untreated cells (Fig. S9*A–F*), and the U75302 treatment downregulated the expression of Acp5, IL-6, IL-1b, and Tnfa when compared to LTB_4-treated cells (Fig. S9*A,D–F*). In addition, the U75302 antagonist did not regulate Nfatc1 and Ctsk when compared to the LTB_4 treatment. (Fig. S9*B,C*).

Discussion

It is known that the production of LTs is stimulated in inflammatory diseases such as RA,[43-45] osteoarthritis,[46,47] and periodontitis,[27,28] and they participate in bone remodeling, acting mainly in the bone resorption process. The importance of our study is based on the fact that a large part of the world population is affected by chronic inflammation-related diseases, such as ischemic heart disease, stroke, cancer, diabetes mellitus, chronic kidney disease (CKD), and autoimmune and neurodegenerative conditions,[48] and the skeletal tissue is vastly affected in those conditions. Understanding the role of LTs in bone metabolism may help in the development of therapeutic strategies concerning the use of LT inhibitors and/or LT receptor antagonists, thus reducing the severity of these diseases and mitigating their symptoms and effects. Our study demonstrated that the 5-LO–deficient mice bone phenotype presents intrinsic differences with respect to WT control mice.

Studies indicated that pharmacological inhibition of 5-LO,[49] as well as 5-LO KO, animals show accelerated fracture healing and bone repair when compared to WT animals.[50,51] Histological sections in a recent study revealed that 5-LO KO mice presented thicker cortical bone in endochondral bones such as the femur and vertebra in comparison to WT mice.[52] Our findings corroborate with these results, showing an increased cortical bone but a larger medullary region in 5-LO–deficient mice as shown in μCT analysis. Interestingly, TNAP and OPN were highly expressed and the number of TNAP-positive and OPN-positive osteoblasts was also higher in the femurs of 5-LO KO mice, but TRAP was expressed lowly; they also had lower numbers of $TRAP^+$ cells and poor osteoclast localization due to a lack of mature osteoclasts in the femur of female 5-LO KO mice when compared to WT mice by IHC analysis of tissue sections. These in vivo results corroborate our in vitro studies on osteoclastogenesis in which 5-LO KO osteoclast precursors did not differentiate into mature osteoclasts.

Importantly, sex differences were identified in our study. Although males and females presented increased cortical bone in the 5-LO KO model, only females had a decreased trabecular bone in comparison with WT littermates. These differences could be explained as due to sex hormones and their relation to LTs biosynthesis and its inhibition. The literature revealed that females are more likely to have 5-LO/5-LO–activating protein (FLAP) complex assembly at the nuclear membrane than males and that male hormones can inhibit the formation of this 5-LO/FLAP complex.[53,54] Another fact is that females could be more susceptible to the development of inflammatory chronic disorders or autoimmune diseases than males.[55] Therefore, the underlying mechanism of these sex-specific effects should be further examined.

This bone structural variation in 5-LO–deficient mice led us to investigate the molecular and functional analysis in vitro, revealing the contribution of these inflammatory mediators in bone homeostasis by affecting osteoblastogenesis and osteoclastogenesis.

The absence of LTs in 5-LO KO animals showed greater potential for osteoblast differentiation and mineralization evidenced by increased ALP activity, a marker of bone formation, and by deposition of calcium in the bone matrix. LT-mediated regulation was further confirmed by the treatment with exogenous LTB_4 and LTD_4, LT inhibitors, and their antagonists. Results showed LT treatment decreased mineralized calcium nodules, whereas the addition of LT inhibitors and their antagonists recovered and/or stimulated the mineralization potential of these cells. Furthermore, 5-LO KO osteoblasts treated exogenously with both LTB_4 and LTD_4 for 21 days under osteogenic conditions presented lower mineralization when compared to untreated 5-LO KO osteoblasts, suggesting that the 5-LO KO mice bone profile is due to the lack of LT production.

The gene expression analysis revealed higher expression of *Alox5* during the WT osteoblast differentiation, and bone formation markers such as *Alpl*, *Bglap*, *Sp7*, *and MMP2* were highly expressed in 5-LO KO osteoblasts. Studies demonstrated that inactivating mutations in the MMP2 gene cause autosomal recessive osteolysis/arthritis syndrome, multicentric osteolysis with arthritis (MOA; MIM #605156) and that the lack of MMP2 decreases bone mineralization.[56] Interestingly, Tnfsf11 was overexpressed in 5-LO KO osteoblasts, perhaps due to compensatory mechanisms. Even though Tnfsf11 was highly expressed in osteoblasts lacking 5-LO, this phenomenon was not correlated to the osteoclast differentiation, which was completely impaired in 5-LO KO mice.

Relatedly, osteogenic markers are upregulated in osteoblasts from 5-LO-KO mice not only on day 10 or 14 but also on almost all time points compared to the osteoblasts from WT mice. These results indicated that LTs are functionally active and might have direct or indirect effects throughout the osteoblast differentiation. However, further studies are needed to completely understand the dynamics of LT signaling during bone remodeling and their mechanisms of action regulating expression of osteogenic factors.

Regarding second messenger cell signaling, the literature demonstrated that intracellular calcium and cAMP are differentially involved in osteogenesis. Although increased calcium levels in osteoblasts induce osteoblast proliferation, differentiation, and mineralization,[57,58] cAMP inhibits mineralization and promotes an osteoclastogenic phenotype in osteoblasts.[59] In this work, 5-LO KO osteoblasts showed higher levels of calcium and lower levels of cAMP compared to WT osteoblasts during cell differentiation, further demonstrating that 5-LO absence is related to a higher osteogenic profile.

We performed proteomic analysis to elucidate possible mechanisms that could explain the differences observed in the bone profile and the intracellular mechanisms of 5-LO KO versus WT mice. All identified proteins and networks are available in the supplemental material (Tables S3 and S4). Thus, some proteins with higher differential expression, such as actin, in its various isoforms, followed by annexin, and peroxiredoxin-1, were decreased by more than two-fold in 5-LO KO osteoblasts. Actin (P60710/P63260- UniProt), is present in the cytoskeleton composition and interacts selectively with adenosine triphosphate (ATP) participating in energy metabolism. Annexin (P07356-UniProt) has an important role as a regulator of the inflammatory process presenting binding properties of cytoskeleton proteins and calcium-dependent phospholipids. In addition, Annexin is a potent inhibitor of phospholipase A2 activity.[60] In the bone context, some annexin isoforms can bind to bone sialoprotein and are also related to the development of osteoclasts. Peroxiredoxin-1 (P35700-UniProt) plays an important role in cellular protection against oxidative stress by detoxifying peroxides and as a sensor of signaling events mediated by hydrogen peroxide.[61] It is also involved in the signaling cascades of growth factors and tumor necrosis factor (TNF)-alpha, regulating intracellular concentrations of H_2O_2.

The downregulation of proteins related to ATP metabolism in 5-LO KO osteoblasts, such as Heat shock 70-kDa protein 1-like (P16627-UniProt), ATP synthase (P56480-Uniprot), and enolases, in their subunits (P17182-Uniprot), indicate a decreased energy

flow in these animals (5-LO KO), which may decrease the oxidative stress. It is known that at low concentrations, the ATP molecule increases bone mineralization.[62] In 5-LO KO osteoblasts, the downregulation of various proteins related to energy metabolism was observed, which could be one of the reasons for the potential increase in mineralization evidenced in animals lacking 5-LO.

Interestingly, cofilins 1/2 (P18760/45591-UniProt) were downregulated in 5-LO KO osteoblasts. These proteins are involved in the depolymerization of actin filaments. A study showed that inhibition of actin depolymerization increases osteoblast differentiation and bone formation.[63] A large class of histones with several subtypes was downregulated in 5-LO KO osteoblasts. Epigenetic studies revealed a relationship between histones methylation processes and osteogenic differentiation, in which high levels of H3K27me3 in the bone morphogenic protein 2 (BMP-2) promoter region are related to the inhibition of osteogenic phenotypes.[64] In addition, most of the proteins identified were unique to 5-LO KO osteoblasts, whereas few were unique to WT cells. Interestingly, prosaposin (Q61207-Uniprot), is known as a precursor for the cleavage of saposins A, B, C, and D, and this protein was found exclusively in 5-LO KO osteoblasts. Saposin-D is a specific sphingomyelin phosphodiesterase[41] activator. A study has shown that sphingomyelin phosphodiesterase 3 (Smpd3) is a key regulator of skeletal development.[41]

In vivo proteomic analysis revealed the AP-1 complex subunit mu-1, which is a vesicular transport adaptor protein localized in the trans-Golgi network (TGN) and endosomes, that regulates the recruitment of clathrin to membranes and the recognition of sorting signals within the cytosolic tails of transmembrane cargo molecules (Uniprot # P35585). The various members of the AP-1 complex are differentially expressed during bone remodeling.[65] Here, we showed that the AP-1 complex was upregulated in long bones from 5-LO KO mice. It is known that matrix vesicles (MVs) are vesicles that can be released from mineralizing cells, such as hypertrophic chondrocytes and osteoblasts, harboring the essential biochemical machinery to induce mineralization.[66] Thus, a possible mechanism that can explain the greater osteogenic profile in 5-LO KO animals is that the upregulation of AP-1 complex in 5-LO KO long bones can enhance the intracellular vesicles transport, which can possibly increase the MVs propagation to the extracellular matrix (ECM) and consequently increase the bone formation in mice lacking 5-LO. However, studies to address the osteogenic profile and the involvement of MVs in 5-LO KO mice need to be done.

Another interesting protein identified was Carbonic anhydrase 1 (CA1), a member of the carbonic anhydrase family, which is involved in the process of bone formation and is susceptible to ankylosing spondylitis, an autoimmune disease characterized by progressive inflammation in the spine and the sacroiliac joints resulting in abnormal bone calcification.[67] Our results from the proteomic analysis revealed exclusive identification of CA1 in the long bones of 5-LO KO mice, but not in WT littermates, emphasizing the importance of proteins related to calcification in the regulation of 5-LO KO mice.

Interleukin 9 receptor was also identified and is a cytokine receptor that specifically mediates the biological effects of interleukin 9 (IL-9), a pleiotropic cytokine, with direct and indirect effects on multiple cell types that influences immune responses and inflammation.[68] IL-9 plays a role in the pathogenesis of chronic inflammatory diseases including bone disorders such as RA. IL-9 was shown to increase osteoclast formation and its function in RA conditions.[69] Our proteomic findings revealed the IL-9 receptor expression exclusive to WT mice, but not in 5-LO KO mice long bones, emphasizing the importance of cytokines for bone resorption. Also, the fusion of mononuclear cells is an important stage during the formation of osteoclasts. A recent study demonstrated that IL-9 regulates the fusion process in osteoclast differentiation by controlling the expression of potassium voltage-gated channel subfamily A member 3 (KCNA3) and cyclin-dependent kinase 6 (CDK6).[70] Here, we showed that 5-LO KO osteoclasts precursors presented impaired fusion capacity, and the lack of IL-9 receptors in those cells may explain this phenomenon.

Several studies demonstrated the role of LTs in bone resorption mediated by osteoclasts. Here we showed that 5-LO KO cells from the monocytic-macrophage lineage did not differentiate in giant and mature osteoclasts, rather they presented a reduced size and nucleation, reduced fusion capacity, impaired resorption function, and decreased cytokines levels compared to WT osteoclasts. Several bone resorption markers were downregulated in cells lacking 5-LO, such as *Acp5*, *c-FOS*, *Tnfsf11*, *Tm7sf4*, and *Sost*. A recent study demonstrated that the downregulation of sclerostin, a potent mineralization inhibitor, promotes bone formation.[71] Inflammatory cytokines such as IL-1b, IL-6, and Tnfa were downregulated in 5-LO KO cells compared to WT osteoclasts. These cytokines are known to stimulate the production of RANKL, and consequently increase osteoclast differentiation.[72] On the contrary, the bone formation marker Opg as well as the Zinc finger and SCAN domain containing 10 (Zscan 10), a transcription factor involved in the suppression of osteoclast differentiation,[73] were upregulated in 5-LO–deficient cells.

A study showed that osteoclasts express BLT1, but not BLT2 receptor, in addition to synthesizing LTB_4. BLT1-Gαi-Rac1 signaling enhances the activation of osteoclasts and the inhibition of BLT1 attenuates the development of diseases related to bone resorption such as osteoporosis.[22] Also, the literature showed that type 1 cysteinyl leukotriene receptor (cysLTR-1) but not type 2 cysteinyl leukotriene receptor (cysLTR-2) is expressed in osteoclast precursors cells and that cysLTR-1 overexpression allowed osteoclast differentiation.[74] Moreover, we showed here that the BLT1 receptor was downregulated in 5-LO KO cells, but CysLT1 expression was not significantly different from WT cells, suggesting the involvement of LTB_4 in osteoclast differentiation.

In summary, this work demonstrated the involvement of LTs in the regulation of bone cells. The absence of 5-LO stimulates bone formation and suppresses bone resorption. Therefore, the comprehension of the mechanisms in which LTs regulate osteoblastogenesis and osteoclastogenesis is critical to understanding the pathophysiology of inflammatory disorders and its impact on skeletal tissue to develop novel therapies for bone-related diseases.

Acknowledgments

This research was supported by the São Paulo Research Foundation (FAPESP), grant numbers 2013/25770-3 to FAO, 2016/23736-0 to CKT, and 2016/08890-3 to RCO. Coordination for the Improvement of Higher Education Personnel (CAPES) fellowship to FAO under grant n. 88881.030354/2013-01 to MARB. The Endocrine Fellows Foundation to FAO. Marie Curie fellowship to FAO from European Union (Programme "PEOPLE"–Call identifier: FP7-PEOPLE-2011-IRSES Proposal No. 295181- Acronym: INTERBONE). We thank

Dr. Ana Paula F. Peti for the assistance with the mass spectrometer sample acquisition for the eicosanoids analysis.

Author Contributions

Flávia Amadeu de Oliveira: Conceptualization; investigation; writing – original draft; validation; writing – review and editing; methodology; visualization; data curation; formal analysis; project administration. **Cintia K. Tokuhara:** Methodology; data curation; writing – original draft. **Vimal Veeriah:** Conceptualization; investigation; writing – original draft; writing – review and editing; formal analysis. **João Paulo Domezi:** Methodology; validation. **Mariana R. Santesso:** Methodology; validation. **Tania M. Cestari:** Methodology; data curation; formal analysis. **Talita M.O. Ventura:** Methodology; validation; data curation; formal analysis. **Adriana A. Matos:** Methodology; data curation. **Thiago Dionísio:** Methodology; data curation. **Marcel R. Ferreira:** Methodology; validation. **Rafael C. Ortiz:** Methodology; data curation. **Marco A.H. Duarte:** Resources. **Marília A.R. Buzalaf:** Resources. **José B. Ponce:** Methodology; formal analysis; data curation. **Carlos A. Sorgi:** Methodology; resources; formal analysis. **Lucia H. Faccioli:** Methodology; resources. **Camila Peres Buzalaf:** Conceptualization; methodology; formal analysis; data curation; supervision; investigation; project administration. **Rodrigo Cardoso de Oliveira:** Conceptualization; writing – review and editing; supervision; resources; funding acquisition; project administration.

Disclosures

The authors declare that there are no conflicts of interest.

Peer Review

The peer review history for this article is available at https://www.webofscience.com/api/gateway/wos/peer-review/10.1002/jbmr.4867.

Data Availability Statement

The data supporting this study's findings are available in this article's supplementary material. Additional data related to this study can be available upon request to the authors.

References

1. Florencio-Silva R, Sasso GR, Sasso-Cerri E, Simões MJ, Cerri PS. Biology of bone tissue: structure, function, and factors that influence bone cells. Biomed Res Int. 2015;2015:421746.
2. Watrous DA, Andrews BS. The metabolism and immunology of bone. Semin Arthritis Rheum. 1989;19(1):45–65.
3. Redlich K, Smolen JS. Inflammatory bone loss: pathogenesis and therapeutic intervention. Nat Rev Drug Discov. 2012;11(3):234–250.
4. Straub RH, Cutolo M, Pacifici R. Evolutionary medicine and bone loss in chronic inflammatory diseases-a theory of inflammation-related osteopenia. Semin Arthritis Rheum. 2015;45(2):220–228.
5. Pasco JA, Henry MJ, Kotowicz MA, et al. Seasonal periodicity of serum vitamin D and parathyroid hormone, bone resorption, and fractures: the Geelong Osteoporosis Study. J Bone Miner Res. 2004;19(5):752–758.
6. Lau EM, Wong SY, Li M, Ma CH, Lim PL, Woo J. Osteoporosis and transforming growth factor-beta-1 gene polymorphism in Chinese men and women. J Bone Miner Metab. 2004;22(2):148–152.
7. Ducy P, Zhang R, Geoffroy V, Ridall AL, Karsenty G. Osf2/Cbfa1: a transcriptional activator of osteoblast differentiation. Cell. 1997;89(5):747–754.
8. Hammarström S. Leukotrienes. Annu Rev Biochem. 1983;52:355–377.
9. Herschman HR. Prostaglandin synthase 2. Biochim Biophys Acta. 1996;1299(1):125–140.
10. Mori S, Jee WS, Li XJ. Production of new trabecular bone in osteopenic ovariectomized rats by prostaglandin E2. Calcif Tissue Int. 1992;50(1):80–87.
11. Miller SC, Marks SC. Alveolar bone augmentation following the local administration of prostaglandin E1 by controlled-release pellets. Bone. 1993;14(3):587–593.
12. Brandt SL, Serezani CH. Too much of a good thing: how modulating LTB4 actions restore host defense in homeostasis or disease. Semin Immunol. 2017;33:37–43.
13. Hoxha M. A systematic review on the role of eicosanoid pathways in rheumatoid arthritis. Adv Med Sci. 2018;63(1):22–29.
14. Wan M, Tang X, Stsiapanava A, Haeggström JZ. Biosynthesis of leukotriene B. Semin Immunol. 2017;33:3–15.
15. Lewis RA, Austen KF, Soberman RJ. Leukotrienes and other products of the 5-lipoxygenase pathway. Biochemistry and relation to pathobiology in human diseases. N Engl J Med. 1990;323(10):645–655.
16. Garcia C, Boyce BF, Gilles J, et al. Leukotriene B4 stimulates osteoclastic bone resorption both in vitro and in vivo. J Bone Miner Res. 1996;11(11):1619–1627.
17. Flynn MA, Qiao M, Garcia C, Dallas M, Bonewald LF. Avian osteoclast cells are stimulated to resorb calcified matrices by and possess receptors for leukotriene B4. Calcif Tissue Int. 1999;64(2):154–159.
18. Traianedes K, Dallas MR, Garrett IR, Mundy GR, Bonewald LF. 5-lipoxygenase metabolites inhibit bone formation in vitro. Endocrinology. 1998;139(7):3178–3184.
19. Funk CD. Prostaglandins and leukotrienes: advances in eicosanoid biology. Science. 2001;294(5548):1871–1875.
20. Collet A, Stewart A. Eicosanoids: physiology update and orthodontic implications. Aust Orthod J. 1991;12:116–123.
21. Paredes Y, Massicotte F, Pelletier JP, Martel-Pelletier J, Laufer S, Lajeunesse D. Study of the role of leukotriene B4 in abnormal function of human subchondral osteoarthritis osteoblasts: effects of cyclooxygenase and/or 5-lipoxygenase inhibition. Arthritis Rheum. 2002;46(7):1804–1812.
22. Hikiji H, Takato T, Shimizu T, Ishii S. The roles of prostanoids, leukotrienes, and platelet-activating factor in bone metabolism and disease. Prog Lipid Res. 2008;47(2):107–126.
23. Moura AP, Taddei SR, Queiroz-Junior CM, et al. The relevance of leukotrienes for bone resorption induced by mechanical loading. Bone. 2014;69:133–138.
24. Jiang J, Lv HS, Lin JH, Jiang DF, Chen ZK. LTB4 can directly stimulate human osteoclast formation from PBMC independent of RANKL. Artif Cells Blood Substit Immobil Biotechnol. 2005;33(4):391–403.
25. Lopes DEM, Jabr CL, Dejani NN, et al. Inhibition of 5-lipoxygenase attenuates inflammation and bone resorption in lipopolysaccharide-induced periodontal disease. J Periodontol. 2017;5:1–18.
26. Klein RF, Allard J, Avnur Z, et al. Regulation of bone mass in mice by the lipoxygenase gene Alox15. Science. 2004;303(5655):229–232.
27. Tsai CC, Hong YC, Chen CC, Wu YM. Measurement of prostaglandin E2 and leukotriene B4 in the gingival crevicular fluid. J Dent. 1998;26(2):97–103.
28. Baroukh B, Saffar JS. The effect of leukotriene synthesis inhibitors on hamster periodontitis. Arch Oral Biol. 1990;35(Suppl):189S–192S.
29. Marzia M, Sims NA, Voit S, et al. Decreased c-Src expression enhances osteoblast differentiation and bone formation. J Cell Biol. 2000;151(2):311–320.
30. Peres CM, Aronoff DM, Serezani CH, Flamand N, Faccioli LH, Peters-Golden M. Specific leukotriene receptors couple to distinct G

proteins to effect stimulation of alveolar macrophage host defense functions. J Immunol. 2007;179(8):5454–5461.

31. Secatto A, Soares EM, Locachevic GA, et al. The leukotriene B_4/BLT_1 axis is a key determinant in susceptibility and resistance to histoplasmosis. PLoS One. 2014;9(1):e85083.
32. Oliveira FA, Matos AA, Matsuda SS, et al. Low level laser therapy modulates viability, alkaline phosphatase and matrix metalloproteinase-2 activities of osteoblasts. J Photochem Photobiol B. 2017;169:35–40.
33. da Silva AP, Petri AD, Crippa GE, Stuani AS, Rosa AL, Stuani MB. Effect of low-level laser therapy after rapid maxillary expansion on proliferation and differentiation of osteoblastic cells. Lasers Med Sci. 2012;27(4): 777–783.
34. Oliveira FA, Matos AA, Santesso MR, et al. Low intensity lasers differently induce primary human osteoblast proliferation and differentiation. J Photochem Photobiol B. 2016;163:14–21.
35. Glocker MO, Guthke R, Kekow J, Thiesen HJ. Rheumatoid arthritis, a complex multifactorial disease: on the way toward individualized medicine. Med Res Rev. 2006;26(1):63–87.
36. Bradford MM. A rapid and sensitive method for the quantitation of microgram quantities of protein utilizing the principle of protein-dye binding. Anal Biochem. 1976;72:248–254.
37. Lima Leite A, Gualiume Vaz Madureira Lobo J, Barbosa da Silva Pereira HA, et al. Proteomic analysis of gastrocnemius muscle in rats with streptozotocin-induced diabetes and chronically exposed to fluoride. PLoS One. 2014;9(9):e106646.
38. Ventura TM, Cassiano LPS, Souza E, et al. The proteomic profile of the acquired enamel pellicle according to its location in the dental arches. Arch Oral Biol. 2017;79:20–29.
39. Ventura TMDS, Ribeiro NR, Dionizio AS, Sabino IT, Buzalaf MAR. Standardization of a protocol for shotgun proteomic analysis of saliva. J Appl Oral Sci. 2018;26:e20170561.
40. Marino S, Logan JG, Mellis D, Capulli M. Generation and culture of osteoclasts. Bonekey Rep. 2014;3:570.
41. Li J, Manickam G, Ray S, et al. Smpd3 expression in both chondrocytes and osteoblasts is required for normal endochondral bone development. Mol Cell Biol. 2016;36(17):2282–2299.
42. Sobue T, Hakeda Y, Kobayashi Y, et al. Tissue inhibitor of metalloproteinases 1 and 2 directly stimulate the bone-resorbing activity of isolated mature osteoclasts. J Bone Miner Res. 2001;16(12):2205–2214.
43. Klickstein LB, Shapleigh C, Goetzl EJ. Lipoxygenation of arachidonic acid as a source of polymorphonuclear leukocyte chemotactic factors in synovial fluid and tissue in rheumatoid arthritis and spondyloarthritis. J Clin Invest. 1980;66(5):1166–1170.
44. Davidson EM, Rae SA, Smith MJ. Leukotriene B4, a mediator of inflammation present in synovial fluid in rheumatoid arthritis. Ann Rheum Dis. 1983;42(6):677–679.
45. Ahmadzadeh N, Shingu M, Nobunaga M, Tawara T. Relationship between leukotriene B4 and immunological parameters in rheumatoid synovial fluids. Inflammation. 1991;15(6):497–503.
46. Pelletier JP, Martel-Pelletier J, Abramson SB. Osteoarthritis, an inflammatory disease: potential implication for the selection of new therapeutic targets. Arthritis Rheum. 2001;44(6):1237–1247.
47. Laufer S. Role of eicosanoids in structural degradation in osteoarthritis. Curr Opin Rheumatol. 2003;15(5):623–627.
48. Furman D, Campisi J, Verdin E, et al. Chronic inflammation in the etiology of disease across the life span. Nat Med. 2019;25(12):1822–1832.
49. Cottrell JA, O'Connor JP. Pharmacological inhibition of 5-lipoxygenase accelerates and enhances fracture-healing. J Bone Joint Surg Am. 2009;91(11):2653–2665.
50. Manigrasso MB, O'Connor JP. Accelerated fracture healing in mice lacking the 5-lipoxygenase gene. Acta Orthop. 2010;81(6):748–755.
51. Cottrell JA, Keshav V, Mitchell A, O'Connor JP. Local inhibition of 5-lipoxygenase enhances bone formation in a rat model. Bone Joint Res. 2013;2(2):41–50.
52. Simionato GB, da Silva ACR, Oliva AH, et al. Lack of 5-lipoxygenase in intramembranous and endochondral 129Sv mice skeleton and intramembranous healing. Arch Oral Biol. 2021;131:105266.
53. Pace S, Sautebin L, Werz O. Sex-biased eicosanoid biology: impact for sex differences in inflammation and consequences for pharmacotherapy. Biochem Pharmacol. 2017;145:1–11.
54. Smith LJ. Leukotrienes and sex: strange bedfellows? J Clin Invest. 2017;127(8):2895–2896.
55. Biguetti CC, Couto MCR, Silva ACR, et al. New surgical model for bone-muscle injury reveals age and gender-related healing patterns in the 5 lipoxygenase (5LO) knockout mouse. Front Endocrinol. 2020;11:484.
56. Mosig RA, Dowling O, DiFeo A, et al. Loss of MMP-2 disrupts skeletal and craniofacial development and results in decreased bone mineralization, joint erosion and defects in osteoblast and osteoclast growth. Hum Mol Genet. 2007;16(9):1113–1123.
57. Dvorak MM, Siddiqua A, Ward DT, et al. Physiological changes in extracellular calcium concentration directly control osteoblast function in the absence of calciotropic hormones. Proc Natl Acad Sci U S A. 2004;101(14):5140–5145.
58. Yamaguchi T, Chattopadhyay N, Kifor O, Sanders JL, Brown EM. Activation of p42/44 and p38 mitogen-activated protein kinases by extracellular calcium-sensing receptor agonists induces mitogenic responses in the mouse osteoblastic MC3T3-E1 cell line. Biochem Biophys Res Commun. 2000;279(2):363–368.
59. Nishihara S, Ikeda M, Ozawa H, Akiyama M, Yamaguchi S, Nakahama KI. Role of cAMP in phenotypic changes of osteoblasts. Biochem Biophys Res Commun. 2018;495(1):941–946.
60. Lima KM, Vago JP, Caux TR, et al. The resolution of acute inflammation induced by cyclic AMP is dependent on annexin A1. J Biol Chem. 2017;292(33):13758–13773.
61. Santos CS, Bannitz-Fernandes R, Lima AS, et al. Monitoring H2O2 inside aspergillus fumigatus with an integrated microelectrode: the role of peroxiredoxin protein Prx1. Anal Chem. 2018;90(4):2587–2593.
62. Cutarelli A, Marini M, Tancredi V, et al. Adenosine triphosphate stimulates differentiation and mineralization in human osteoblast-like Saos-2 cells. Dev Growth Differ. 2016;58(4):400–408.
63. Chen L, Shi K, Frary CE, et al. Inhibiting actin depolymerization enhances osteoblast differentiation and bone formation in human stromal stem cells. Stem Cell Res. 2015;15(2):281–289.
64. Yoon DK, Park JS, Rho GJ, et al. The involvement of histone methylation in osteoblastic differentiation of human periosteum-derived cells cultured in vitro under hypoxic conditions. Cell Biochem Funct. 2017;35(7):441–452.
65. Wagner EF, Eferl R. Fos/AP-1 proteins in bone and the immune system. Immunol Rev. 2005;208:126–140.
66. Bottini M, Mebarek S, Anderson KL, et al. Matrix vesicles from chondrocytes and osteoblasts: their biogenesis, properties, functions and biomimetic models. Biochim Biophys Acta Gen Subj. 2018; 1862(3):532–546.
67. Chang X, Zheng Y, Yang Q, et al. Carbonic anhydrase I (CA1) is involved in the process of bone formation and is susceptible to ankylosing spondylitis. Arthritis Res Ther. 2012;14(4):R176.
68. Goswami R, Kaplan MH. A brief history of IL-9. J Immunol. 2011; 186(6):3283–3288.
69. Chakraborty S, Schneider J, Mitra DK, Kubatzky KF. Mechanistic insight of interleukin-9 induced osteoclastogenesis. Immunology. 2023;169(3):309–322.
70. Kar S, Gupta R, Malhotra R, et al. Interleukin-9 facilitates osteoclastogenesis in rheumatoid arthritis. Int J Mol Sci. 2021;22(19):10397.
71. Zhang ZH, Jia XY, Fang JY, et al. Reduction of SOST gene promotes bone formation through the Wnt/β-catenin signalling pathway and compensates particle-induced osteolysis. J Cell Mol Med. 2020;24(7):4233–4244.
72. Xiao W, Wang Y, Pacios S, Li S, Graves DT. Cellular and molecular aspects of bone remodeling. Front Oral Biol. 2016;18:9–16.
73. Yanagihara Y, Inoue K, Saeki N, et al. Zscan10 suppresses osteoclast differentiation by regulating expression of Haptoglobin. Bone. 2019;122:93–100.
74. Zheng C, Shi X. Cysteinyl leukotriene receptor 1 (cysLT1R) regulates osteoclast differentiation and bone resorption. Artif Cells Nanomed Biotechnol. 2018;46(sup3):S64–S70.